Groupwise Frequency Domain Multiuser MMSE Turbo Equalization for Single Carrier Block Transmission over Spatially-Correlated Channels

Marcus Grossmann and Christian Schneider

***Abstract*—This paper proposes a novel turbo equalization scheme based on *groupwise* soft interference cancelling minimum mean-squared error filtering (SC-MMSE) combined with maximum *a posteriori* signal detection for multiple access single-carrier block transmission. For an efficient implementation of the equalizer, the linear *groupwise* SC-MMSE filter is directly derived in the frequency domain by introducing an additional design criterion in the optimization. Special focus is given on different heuristic methods for group selection based on mean-squared error (MSE) and spatial channel correlation criteria. The first method dynamically forms groups incorporating *a priori* information at each turbo iteration, while the second and third methods provide a static grouping that is valid for all turbo iterations. Results of correlation chart analysis and bit error rate simulations demonstrate that the *groupwise* turbo frequency domain equalizer (FDE) achieves a large performance gain over the conventional SC-MMSE FDE in intersymbol interference multiple access channels with high spatial correlation among the multiple users' transmitted signals. Moreover, it is shown that the simple static correlation-based grouping scheme when applied to the proposed receiver achieves similar performance than the dynamic MSE-based scheme at a significantly reduced complexity. In addition, to assess the practicality of the novel algorithm in real scenarios, we show numerical results obtained by a series of simulations using channel-sounding field measurement data.**

***Index Terms*—*groupwise* minimum mean-squared error turbo equalization, spatially correlated channels, correlation chart analysis, single carrier transmission**

I. Introduction

Turbo equalization [2]-[19] is a joint channel equalization/signal detection and decoding technique used for multiuser *single-carrier* communication systems with coded data transmissions over intersymbol-interference (ISI) multiple-access fading channels. By iteratively exchanging probabilistic information about the code bits between a soft-input soft-output (SfiSfo) channel equalizer/multiuser detector and a bank of SfiSfo channel decoders, the turbo equalizer can achieve near-optimal performance at very low computational complexity compared to optimal multiuser detection [1]. In its primal form, Douillard *et al.* [2] involved the *maximum a posteriori* probability (MAP) algorithm for iterative joint equalization and decoding. However, owing to the exponential increase in computational complexity, such a MAP-based turbo equalizer is only applicable for systems with a moderate number of users, transmissions with simple modulation formats, like binary phase shift keying (BPSK), and ISI channels with few multipath components. Recently, linear filter-based turbo equalizers utilizing the minimum mean-squared error (MMSE) criterion have attracted considerable interest [3]-[19]. In this regard, Wang and Poor [3] proposed an iterative detection scheme for random coded code-division multiple-access (CDMA) systems that replaces the optimal MAP algorithm by a low-cost alternative utilizing a combination of a soft interference canceler and a time-varying (conditional) linear MMSE filter (SC-MMSE), whose coefficients are calculated for every transmitted data symbol based on the available *a priori* knowledge from channel decoding. The SC-MMSE-based turbo approach of [3], with a cubic complexity in all system parameters, has been later applied by Tüchler *et al.* [4] to iterative equalization of single-user coded transmission with ISI, and further extended by Abe *et al.* to multiple-input multiple-output (MIMO) channel equalization in [6]. In [7]-[11], it has been shown that SC-MMSE block-based frequency domain equalization (SC-MMSE FDE) allows further reduction in computational complexity by exploiting the circulant structure of the channel matrices, obtained when resorting to a cyclic prefix-based (CP) transmission scheme. More specifically, the SC-MMSE FDE was derived by applying the equal variance approximation [10], [12] on the coded data symbols, yielding time-invariant filter coefficients, and converting the MMSE equation into the frequency domain.

Unfortunately, due to its simplicity, the conventional SC-MMSE-based turbo receiver suffers from a considerable performance loss, e.g., as shown in [16] for orthogonal frequency division multiplexing (OFDM) multiuser transmission, when applied to the ISI multiple access spatially-correlated fading channel. To overcome this performance degradation, *groupwise* turbo equalization [15], [16] can be employed that combines SC-MMSE filtering and optimal MAP detection.

The idea of *groupwise* multiuser detection was first introduced by Varanasi in [20] for uncoded code division multiple-access (CDMA) channels. The group detector (GD) partitions the users' signals into a set of disjoint subgroups, and then employs the maximum likelihood detection sequentially or in parallel to the signals in each subgroup. Compared to the

This work was supported in part by the German Research Foundation (DFG) under grant SPP1163 and the Ultra high-speed Mobile Information and Communication (UMIC) research centre under the German Federal and State Government excellence initiative.

Marcus Grossmann has been with the Institute for Information Technology, Ilmenau University of Technology, 98684 Ilmenau, Germany. He is now with the Fraunhofer Institute for Integrated Circuits, 98684 Ilmenau, Germany (e-mail: marcus.grossmann@iis.fraunhofer.de).

Christian Schneider is the Institute for Information Technology, Ilmenau University of Technology, 98684 Ilmenau, Germany (e-mail: christian.schneider@tu-ilmenau.de).

optimal solution, the GD achieves near-optimal performance at a significantly reduced complexity. The concept from [20] was extended in [21] to group antenna detection (GAD) using linear subspace processing for inter-group interference (IGI) suppression of spatially-multiplexed MIMO channels with frequency-flat fading. Also, the authors of [21] presented a channel correlation-based group selection (GS) scheme that optimizes the grouping for each individual antenna with respect to optimum system performance. Among other contributions, Moon *et. al.* [22] has recently shown that the GAD scheme [21] can be further improved when taking into account the noise statistics at the receiver. Particularly, they proposed a group separation strategy based on *groupwise* linear filtering maximizing the signal-to-interference-plus-noise ratio (SINR) in each subgroup. In addition, the authors showed that the SINR criteria can be efficiently be used to derive an SINR-based GS method that maximizes performance.

Several group detectors employing turbo processing for a coded data transmission were presented in [14]-[17]. Iterative soft interference cancellation combined with noise-whitening filtering, incorporating *a priori* information from channel decoding, was used in [14] to group detection for MIMO flat-fading systems having more transmitter than receiver antennas. Note that due to presence of the decoder feedback, the receiver involves MAP instead of ML detection. In [15], Veselinovic *et al.* considered a space-time trellis-coded (STTrC) system in multiple-access ISI fading channels and derived a time-domain *groupwise* SC-MMSE filtering technique for joint signal detection of multiple transmit antennas. The aim of jointly detecting symbols from different antennas was to preserve the effective degrees of freedom used for suppression of unknown co-channel interfering signals. In [16], the authors extended the *groupwise* SC-MMSE approach from [15] to OFDM multiuser systems with iterative detection. Group equalization combining frequency domain SC-MMSE filtering and MAP symbol detection has also been considered in [17]. However, unlike to the *groupwise* filtering approach [15], [16], the MMSE block from [17] performs the suppression of residual interferences on a *user-by-user* basis, similar to the standard MMSE filter [4], to separate the transmitted signals. The MSE at the equalizer output can therefore not be used to evaluate the performance of each subgroup which is needed for an adaptive GS at each turbo iteration.

In this paper, we consider the joint channel equalization/multiuser signal detection problem for coded single-carrier multiple access transmission over ISI channels. Our goal is to design a computationally efficient turbo receiver that is robust against spatial channel correlation. To achieve this goal, we adapt the group detection strategy from [20] and extend the standard SC-MMSE FDE to a hybrid equalizer that performs frequency domain *groupwise* processing of the multiple users' transmitted symbols. In particular, the proposed algorithm divides the users' signals into several non-overlapping subgroups and performs IGI equalization utilizing *groupwise* SC-MMSE filtering. The objective of the *groupwise* filter is to *jointly* suppress residual interferences for the users' signals in each subgroup. In contrast to previous work [7]-[12], [17], we directly derive the MMSE filtering block in the frequency domain to reduce the complexity for the covariance matrix inversions involved in SC-MMSE equalization.

Particular emphasis is put in this paper on the grouping strategy which mainly determines the overall performance of the system. Three greedy algorithms based on MSE and correlation criteria for grouping the users into several subgroups are proposed. The aim of these algorithms is to find groupings that reduce noise enhancement due to the SC-MMSE interference suppression of highly correlated user signals. The first scheme dynamically forms subgroups at each turbo iteration by computing among all possible group partitions the one that minimizes the maximum subgroup's MSE. The calculation of each partition involves a number of matrix inversions, which however, limits the application of the dynamic MSE-based algorithm to systems with a small number of users. The second and third schemes reduce complexity by providing a static grouping that is valid for all turbo iterations. It is shown that the simple static correlation-based algorithm outperforms the static MSE-based grouping scheme and achieves similar performance than the dynamic MSE-based algorithm at a significantly reduced complexity when applied to the proposed turbo receiver.

To quantify the merit of the *groupwise* equalizer, we compare its convergence properties with the standard SC-MMSE FDE using the correlation chart analysis [13]. Moreover, we evaluate its bit error rate (BER) and frame error rate (FER) performance in Rayleigh fading ISI channels with predefined fixed spatial correlations. In addition, to assess the practicality of the novel scheme in real scenarios, we show numerical results obtained by a series of simulations using channel-sounding field measurement data.

The rest of this paper is organized as follows. In Section II the system and channel model are introduced. A full derivation of the proposed turbo equalizer is presented in Section III. In Section IV, we propose three different greedy methods for the problem of grouping the users into a set of subgroups. The convergence property analysis is provided in Section V. In Section VI, we present some numerical results to verify the performance of the novel schemes. Finally, we summarize our results in Section VII.

Throughout this paper, the following notations are adopted. Normal letters represent scalar quantities, boldface lower case and boldface uppercase letters designate vectors and matrices, respectively. The transpose and conjugate transpose operators are denoted by $(\cdot)^T$ and $(\cdot)^H$, respectively. The (l,k)th entry of a matrix $\mathbf{A}$ is denoted by $[\mathbf{A}]_{l,k}$. The $Q \times Q$ identity matrix and the $Q \times 1$ all-one vector are denoted by $\mathbf{I}_Q$ and $\mathbf{1}_Q$, respectively. The vector $\mathbf{e}_k$ is the all-zero column vector with the kth entry being one. The $\mathrm{circ}_Q\{\mathbf{a}\}$ operator generates an $Q \times Q$ circulant matrix having the elements of vector $\mathbf{a}$ on its first column. The symbol $\otimes$ indicates the Kronecker product. The operator $\mathrm{diag}\{\mathbf{A}\}$ extracts the diagonal elements of a square matrix $\mathbf{A}$. The operator $\mathrm{diag}\{\mathbf{a}\}$ generates a square diagonal matrix having the elements of vector $\mathbf{a}$ on its diagonal, whereas the operator $\mathrm{ddiag}\{\mathbf{A}\}$ generates a diagonal matrix having the diagonal elements of $\mathbf{A}$ on its main diagonal. Finally, $\mathrm{Trace}(\cdot)$ and $\mathbb{E}[\cdot]$ denote the trace operator and expectation, respectively.

II. System Model

We consider a synchronous single carrier cyclic prefix (CP) assisted multiuser uplink system with N active users, each equipped with a single transmit antenna. The receiver is equipped with M antennas. The transmission scheme of the nth user ($n = 1, .., N$) is based on bit-interleaved coded modulation (BICM), where the information bits are organized in frames. Each frame consists of N_I bits, arranged in a vector $\mathbf{u}_n$, which is first encoded by a rate-r_c binary encoder, yielding the coded bit vector $\mathbf{a}_n$. The encoded bit vector $\mathbf{a}_n$ is interleaved by a random bit-interleaver, and BPSK modulated[1]. The binary encoder is a serially concatenated convolutional code (SCCC) [32] and identical for all users. After symbol mapping, the BPSK modulated data sequence at the nth user is grouped into K equal-sized blocks, each containing Q BPSK symbols, $\mathbf{b}_n(k) \equiv \big[b_{0,n}(k), ..., b_{q,n}(k), ..., b_{Q-1,n}(k)\big]^T$, $k = 1, .., K$. These blocks are transmitted simultaneously from the N users over the frequency-selective fading MIMO channel. Note that throughout the paper, we use index n to denote user n.

The channel impulse response (CIR) between the nth user's transmit antenna and the mth receive antenna is denoted by $\mathbf{h}_{n,m} \equiv \big[h_{n,m}(0), ..., h_{n,m}(l), ..., h_{n,m}(L-1)\big]^T$, where L is the channel memory length that is assumed to be identical for all links. The block-grouping of the transmit data symbols is assumed to be aligned with the channel coherence time such that the channel coefficients $h_{n,m}(l)$ can reasonable be regarded as being time-invariant during the transmission of a complete frame of K subsequently transmitted blocks. This inherently leads to the assumption of a so called (quasi-) static MIMO channel. Moreover, we always assume that the N transmitters and the receiver are perfectly synchronized and all channel gains are known at the receiver. For the simulations using the statistical channel model, the MIMO channel matrices are generated according to a spatially-correlated Rayleigh fading distribution. The spatial correlation matrices follow the well-known Kronecker model [23] and are assumed to be identical for all channel taps, i.e,

$$\mathbb{E}\big[\hat{\mathbf{H}}_l^H \hat{\mathbf{H}}_l\big] \equiv \mathbf{S}, l = 0, .., L-1,$$
$$\mathbb{E}\big[\hat{\mathbf{H}}_l \hat{\mathbf{H}}_l^H\big] \equiv \mathbf{R}, l = 0, .., L-1,$$

where $\hat{\mathbf{H}}_l$ denotes the $M \times N$ channel matrix corresponding the lth delay-tap, and $\mathbf{S} \in \mathbb{C}^{N\times N}$ and $\mathbf{R} \in \mathbb{C}^{M\times M}$ are the spatial transmit and receive correlation matrices, respectively. For simplicity, we assume uncorrelated receive antennas here with identical radiation pattern, such that $\mathbf{R} = \mathbf{I}_M$.

For an efficient implementation of the frequency-domain filtering at the receiver, each data block $\mathbf{b}_n(k)$ is preceded by a CP of length $P = L-1$ before transmission, where the CP is a copy of the last P symbols of the block. After removal of the CP at the receiver, the signals from the M antennas are arranged into $QM \times 1$ vectors $\mathbf{r}(k)$, $k = 1, .., K$. These vectors are given by

$$\mathbf{r}(k) = \sum_{n=1}^{N} \mathbf{H}_n \mathbf{b}_n(k) + \mathbf{n}(k), k = 1, .., N, \qquad (1)$$

where $\mathbf{H}_n = [\mathbf{H}_{n,1}^T, ..., \mathbf{H}_{n,m}^T, ..., \mathbf{H}_{n,M}^T]^T \in \mathbb{C}^{MQ\times Q}$ is the block-circulant channel matrix associated to the n-th user with $\mathbf{H}_{n,m} = \text{circ}_Q\big\{\mathbf{h}_{n,m}\big\} \in \mathbb{C}^{Q\times Q}$, and $\mathbf{n}(k) \sim \mathcal{CN}(\mathbf{0}, \sigma_0^2\mathbf{I})$ is the additive white Gaussian noise (AWGN). It is well known that the eigenvalue decomposition of $\mathbf{H}_n$ can be expressed as [10]

$$\mathbf{H}_n = \mathbf{F}_M^H \mathbf{\Xi}_n \mathbf{F}, \qquad (2)$$

where $\mathbf{F}_M \equiv (\mathbf{I}_M \otimes \mathbf{F})$ is the block-Fourier matrix with $\mathbf{F}$ being the Q-point discrete Fourier transform (DFT) matrix, whose (l, j)-th element is given by $1/\sqrt{Q}e^{-\sqrt{-1}\frac{2\pi}{Q}lj}$, $0 \le l, j \le Q-1$, and $\mathbf{\Xi}_n$ is the block-diagonal frequency domain channel matrix.

An iterative joint channel equalization and decoding structure is employed at the receiver. The equalizer and the N single-user channel decoders exchange *extrinsic* log likelihood ratios (LLRs) of the coded bits. We denote by $\lambda_{(\cdot)}[\cdot]$ and $\zeta_{(\cdot)}[\cdot]$ the *extrinsic* and the *a priori* LLR, respectively, where the subscript $(\cdot)$ is used to distinguish between the components of the receiver.

The iterative equalizer deals jointly with the channel equalization, the user-signal detection and the symbol-wise demapping. Its aim is to mitigate inter-symbol interference (ISI) and to cancel multiple-access interference (MAI) caused by the multiple-transmit data streams of the N users. It processes the received signals $\mathbf{r}(k)$ and the *a priori* information sequences

$$\big\{\zeta_e[b_{q,n}(k)] | q = 0, ..., Q-1, n = 1, ..., N, k = 1, ...K\big\}$$

about the code bits from all users, where

$$\zeta_e[b_{q,n}(k)] \equiv \log\left(\frac{\text{Prob}\big(b_{q,n}(k) = +1\big)}{\text{Prob}\big(b_{q,n}(k) = -1\big)}\right),$$

and outputs the *extrinsic* LLRs $\lambda_e[b_{q,n}(k)]$ for all transmitted bits $b_{q,n}(k)$. We remark that during the first iteration of turbo equalization, $\zeta_e[b_{q,n}(k)]$ is zero for all n, q, k. Later on, it is provided in the form of the *extrinsic* LLRs $\lambda_d[a_n(i)]$ from the channel decoder. The *extrinsic* LLRs $\lambda_e[b_{q,n}(k)]$ are forwarded via the deinterleavers to the bank of N single-user decoders and serve there in the next turbo iteration as *a priori* information $\zeta_d[a_n(i)]$ about the code bits $a_n(i)$.

III. Hybrid Soft Cancellation Frequency Domain MMSE Equalization

In this section, we establish the equalizer structure for the proposed hybrid turbo scheme. The new equalizer separates the transmitted signals into G *disjoint* subgroups, labeled by the sets $(\mathcal{A}_1, ..., \mathcal{A}_g, ..., \mathcal{A}_G)$, such that each subgroup $\mathcal{A}_g = \{a_1, ..., a_U\}$, $a_1 < .... < a_U$ contains U integers corresponding to indexes of users that are jointly detected[2]. Without

[1]Note that in this paper, we only consider BPSK modulation, however, the extension to more generic modulation formats is rather straightforward.

[2]Note that the proposed scheme can easily be extended to group detection with overlapping subgroups.

loss of generality, we assume identical sized subgroups, such that $N = GU$.

Consider equalization of the transmitted signals from the U users of the gth subgroup and kth data block. Correspondingly, the received signals can be split into two parts: the first part contains the transmitted signals from the users of the desired gth subgroup and the second part contains the interference components from the remaining $G-1$ subgroups and the additive Gaussian noise. By denoting $\mathbf{c}_g(k) \equiv [\mathbf{b}_{a_1}^T(k), ..., \mathbf{b}_{a_u}^T(k), ..., \mathbf{b}_{a_U}^T(k)]^T$, $\forall a_u \in \mathcal{A}_g$ as the vector containing the users' transmitted signals of the gth subgroup, we can rewrite (1) as

$$\mathbf{r}(k) = \overline{\mathbf{H}}_g \mathbf{c}_g(k) + \sum_{j=1, j\neq g}^{G} \overline{\mathbf{H}}_j \mathbf{c}_j(k) + \mathbf{n}(k), \tag{3}$$

where $\overline{\mathbf{H}}_g \equiv [\mathbf{H}_{a_1}, ..., \mathbf{H}_{a_u}, ..., \mathbf{H}_{a_U}] \in \mathbb{C}^{QM \times QU}$, $a_u \in \mathcal{A}_g$ is the gth subgroup's channel matrix. Here, the term $\sum_{j=1, j\neq g}^{G} \overline{\mathbf{H}}_j \mathbf{c}_j(k)$ denotes the interference components from $G-1$ non-desired subgroups. For a compact notation of (3), we define

$$\overline{\overline{\mathbf{H}}}_g \equiv [\overline{\mathbf{H}}_1, ..., \overline{\mathbf{H}}_{g-1}, \overline{\mathbf{H}}_{g+1}, ..., \overline{\mathbf{H}}_G], 1 \leq g \leq G \tag{4}$$

and

$$\mathbf{d}_g(k) \equiv [\mathbf{c}_1^T(k), ..., \mathbf{c}_{g-1}^T(k), \mathbf{c}_{g+1}^T(k), ..., \mathbf{c}_G^T(k)]^T, 1 \leq g \leq G \tag{5}$$

as the matrix and the vector containing all users' channels and all users' transmitted signals, respectively, except those from the gth subgroup. Based on (4) and (5), Eqn. (3) can be compactly written as

$$\mathbf{r}(k) = \overline{\mathbf{H}}_g \mathbf{c}_g(k) + \overline{\overline{\mathbf{H}}}_g \mathbf{d}_g(k) + \mathbf{n}(k). \tag{6}$$

A. Derivation of Frequency Domain Filter Coefficients

The equalizer performs soft interference cancellation and frequency domain MMSE filtering for *groupwise* separation of the users' transmitted signals. Specifically, following the standard SC-MMSE approach [3], it uses the available *a priori* LLR information $\{\zeta_e[b_{q,n}(k)] | q = 0, ..., Q-1, n = 1, ..., N, k = 1, ...K\}$ to compute soft-estimates $\bar{b}_{q,n}(k) = \mathbb{E}[b_{q,n}(k) | \zeta_e[b_{q,n}(k)]]$ for each transmitted symbol $b_{q,n}(k)$ using the conditional mean estimator. With the use of a sufficiently long random bit-interleaver at each user, it can be assumed that the values $\bar{b}_{k,q}(n)$ are mutually uncorrelated. Then, it holds that [24]

$$\begin{aligned} \mathbb{E}[\bar{b}_{q,n}(k)\bar{b}_{i,j}(l)] &= \mathbb{E}[b_{q,n}(k)\bar{b}_{i,j}(l)] \\ &= 0 \text{ for } (q,n,k) \neq (i,j,l). \end{aligned} \tag{7}$$

The soft-estimates are used to construct a soft replica of the gth subgroup's desired signals and the interference components as

$$\mathbf{s}(k) = \overline{\mathbf{H}}_g \bar{\mathbf{c}}_g(k) + \overline{\overline{\mathbf{H}}}_g \bar{\mathbf{d}}_g(k), \tag{8}$$

where $\bar{\mathbf{c}}_g(k)$ and $\bar{\mathbf{d}}_g(k)$ are the conditional mean of $\mathbf{c}_g(k)$ and $\mathbf{d}_g(k)$, respectively.

Given the soft replica (8), the hybrid equalizer performs soft interference cancellation and linear groupwise MMSE filtering of the received signal $\mathbf{r}(k)$ to separate the transmitted signals into G independent subgroups. In contrast to the standard SC-MMSE approach that performs ISI/MAI cancellation on a user-by-user basis, the groupwise MMSE filter suppresses all residual interference components from non-desired subgroups as well as the desired subgroup's residual ISI components, while preserving the effective degrees of freedom of the desired subgroup's spatial components for joint signal MAP detection.

Let us define by $\mathbf{W}_g \equiv [\mathbf{W}_{g,1}, ..., \mathbf{W}_{g,u}, ..., \mathbf{W}_{g,U}]$, $1 \leq g \leq G$ the filtering matrix for the gth subgroup of size $QM \times QU$, where each sub-matrix $\mathbf{W}_{g,u} \equiv [\mathbf{W}_{g,u,1}^H, ..., \mathbf{W}_{g,u,m}^H, ..., \mathbf{W}_{g,u,M}^H]^H$, $\mathbf{W}_{g,u,m} \in \mathbf{C}^{Q \times Q}$ defines the filter matrix corresponding to the uth user. Based on the modified system model in (6), the filter output signal at the gth subgroup, which is an estimate of $\mathbf{c}_g(k)$, can be expressed as

$$\begin{aligned} \mathbf{z}_g(k) &= \mathbf{W}_g^H \big(\mathbf{r}(k) - \mathbf{s}(k)\big) + \mathbf{M}_g \bar{\mathbf{c}}_g(k) \\ &= \mathbf{M}_g \mathbf{c}_g(k) + (\mathbf{W}_g^H \overline{\mathbf{H}}_g - \mathbf{M}_g)\big(\mathbf{c}_g(k) - \bar{\mathbf{c}}_g(k)\big) \\ &\quad + \mathbf{W}_g^H \overline{\overline{\mathbf{H}}}_g \big(\mathbf{d}_g(k) - \bar{\mathbf{d}}_g(k)\big) + \mathbf{W}_g^H \mathbf{n}(k), \end{aligned} \tag{9}$$

where $\mathbf{M}_g \in \mathbb{C}^{QU \times QU}$ is the equivalent channel matrix after *groupwise* MMSE filtering,

$$\mathbf{M}_g \equiv \begin{bmatrix} \mathbf{M}_{g,1,1} & \dots & \mathbf{M}_{g,1,U} \\ \vdots & \ddots & \vdots \\ \mathbf{M}_{g,U,1} & \dots & \mathbf{M}_{g,U,U} \end{bmatrix} \tag{10}$$

with $\mathbf{M}_{g,i,j} \in \mathbb{C}^{Q \times Q}$, $1 \leq i, j \leq U$ being diagonal sub-matrices, whose entries are given by

$$\mathbf{M}_{g,i,j} \equiv \text{ddiag}\{\mathbf{W}_{g,i}^H \mathbf{H}_{a_j}\}.$$

Note that in (9) the first term represents the received signal of the desired gth subgroup, the second term represents the residual self-interference components from all users within the gth subgroup, the third term represents the residual interference components from the users' signals of the remaining $G-1$ subgroups ($j \neq g$), and the last term represents filtered additive Gaussian noise.

Design criterion 3.1. *For an efficient implementation of the linear filtering equation (9) in the frequency domain, the filtering matrix $\mathbf{W}_g$ is constrained to be block-circulant.*

With design criterion 3.1, similar to (2), we can write

$$\mathbf{W}_g = \mathbf{F}_M^H \mathbf{\Gamma}_g \mathbf{F}_U, \tag{11}$$

where $\mathbf{\Gamma}_g \equiv [\mathbf{\Gamma}_{g,1}, ..., \mathbf{\Gamma}_{g,u}, ..., \mathbf{\Gamma}_{g,U}] \in \mathbb{C}^{QM \times QU}$ is the frequency domain filtering matrix, consisting of sub-matrices $\mathbf{\Gamma}_{g,u} \equiv [\mathbf{\Gamma}_{g,u,1}^H, ..., \mathbf{\Gamma}_{g,u,m}^H, ..., \mathbf{\Gamma}_{g,u,M}^H]^H$ with $\mathbf{\Gamma}_{g,u,m} \in \mathbb{C}^{Q \times Q}$ being a diagonal matrix. Here the entry $[\Gamma_{g,u,m}]_{q,q}$ denotes the gth subgroup's filter coefficient at frequency-bin q for user/receive antenna pair (a_u, m), $a_u \in \mathcal{A}_g$. By applying the matrix decomposition (11) to (9), the linear filtering equation can be converted into the frequency domain,

$$\begin{aligned} \underline{\mathbf{z}}_g(k) &\equiv \mathbf{F}_U \mathbf{z}_g(k) \\ &= \mathbf{M}_g \underline{\mathbf{c}}_g(k) + (\mathbf{\Gamma}_g^H \overline{\mathbf{\Xi}}_g - \mathbf{M}_g)(\underline{\mathbf{c}}_g(k) - \bar{\underline{\mathbf{c}}}_g(k)) \\ &\quad + \mathbf{\Gamma}_g^H \overline{\overline{\mathbf{\Xi}}}_g (\underline{\mathbf{d}}_g(k) - \bar{\underline{\mathbf{d}}}_g(k)) + \mathbf{\Gamma}_g^H \underline{\mathbf{n}}(k), \end{aligned} \tag{12}$$

where $\overline{\boldsymbol{\Xi}}_g = [\boldsymbol{\Xi}_{a_1}, ..., \boldsymbol{\Xi}_{a_u}, ..., \boldsymbol{\Xi}_{a_U}]$, $a_u \in \mathcal{A}_g$, $1 \le g \le G$ is the gth subgroup's frequency domain channel matrix, $\overline{\overline{\boldsymbol{\Xi}}}_g = [\overline{\boldsymbol{\Xi}}_1, ..., \overline{\boldsymbol{\Xi}}_{g-1}, \overline{\boldsymbol{\Xi}}_{g+1}, ..., \overline{\boldsymbol{\Xi}}_G]$, and $\underline{\mathbf{c}}_g(k) = \mathbf{F}_U \mathbf{c}_g(k)$, $\underline{\bar{\mathbf{c}}}_g(k) = \mathbf{F}_U \bar{\mathbf{c}}_g(k)$, $\underline{\mathbf{d}}_g(k) = \mathbf{F}_{N-U} \mathbf{d}_g(k)$, $\underline{\bar{\mathbf{d}}}_g(k) = \mathbf{F}_{N-U} \bar{\mathbf{d}}_g(k)$, and $\underline{\mathbf{n}}(k) = \mathbf{F}_M \mathbf{n}(k)$. Moreover, using (11), we can also write (10) as

$$\mathbf{M}_g = \mathbf{F}_U^H \mathbf{M}_g \mathbf{F}_U = \mathbf{U}_g \otimes \mathbf{I}_Q,$$

where $\mathbf{U}_g \in \mathbb{C}^{U \times U}$ with the (i,j)th element being given as $[\mathbf{U}_g]_{i,j} = Q^{-1}\text{Trace}\big(\boldsymbol{\Gamma}_{g,i} \boldsymbol{\Xi}_{a_j}\big)$, $1 \le i, j \le U$, $a_j \in \mathcal{A}_g$.

Design criterion 3.2. *The groupwise frequency domain filter $\boldsymbol{\Gamma}_g$ should minimize the average unconditional (i.e., ensemble averaged) linear mean-squared error (MSE) between the gth subgroup's transmitted signals and the frequency domain filter output signal (12),*

$$\text{MSE}_g \equiv Q^{-1}\mathbb{E}\big[\, \big\|\underline{\mathbf{z}}_g(k) - \mathbf{M}_g \underline{\mathbf{c}}_g(k)\big\|^2 \,\big]. \tag{13}$$

Defining $\boldsymbol{\Sigma}$ as the covariance matrix of the soft cancellation (frequency domain) output vector $\underline{\check{\mathbf{r}}}(k) \equiv \mathbf{F}_M(\mathbf{r}(k) - \mathbf{s}(k))$,

$$\begin{aligned}\boldsymbol{\Sigma} &\equiv \mathbb{E}\big[\underline{\check{\mathbf{r}}}(k)\underline{\check{\mathbf{r}}}^H(k)\big] \\ &= \overline{\boldsymbol{\Xi}}_g \boldsymbol{\Lambda}_g^{(1)} \overline{\boldsymbol{\Xi}}_g^H + \overline{\overline{\boldsymbol{\Xi}}}_g \boldsymbol{\Lambda}_g^{(2)} \overline{\overline{\boldsymbol{\Xi}}}_g^H + \sigma_0^2 \mathbf{I}\end{aligned}$$

with $\boldsymbol{\Lambda}_g^{(1)}$ and $\boldsymbol{\Lambda}_g^{(2)}$ being the covariance matrices of the vectors $\underline{\mathbf{c}}_g(k)$ and $\underline{\mathbf{d}}_g(k)$, respectively,

$$\boldsymbol{\Lambda}_g^{(1)} \equiv \mathbb{E}\Bigg[\mathbb{E}\Big[\, \big(\underline{\mathbf{c}}_g(k) - \underline{\bar{\mathbf{c}}}_g(k)\big)\big(\underline{\mathbf{c}}_g(k) - \underline{\bar{\mathbf{c}}}_g(k)\big)^H \Big| \big\{\zeta_e[b_{q,j}(k)], j \in \mathcal{A}_g, \forall q, k\big\}\Big]\Bigg], \tag{14}$$

$$\boldsymbol{\Lambda}_g^{(2)} \equiv \mathbb{E}\Bigg[\mathbb{E}\Big[\, \big(\underline{\mathbf{d}}_g(k) - \underline{\bar{\mathbf{d}}}_g(k)\big)\big(\underline{\mathbf{d}}_g(k) - \underline{\bar{\mathbf{d}}}_g(k)\big)^H \Big| \big\{\zeta_e[b_{q,j}(k)], j \in \mathcal{A}_l, j \ne g, \forall q, k\big\}\Big]\Bigg], \tag{15}$$

the MSE can be written as

$$\begin{aligned}\text{MSE}_g &= Q^{-1}\text{Trace}\Big(\boldsymbol{\Gamma}_g^H \boldsymbol{\Sigma} \boldsymbol{\Gamma}_g - \boldsymbol{\Gamma}_g^H \overline{\boldsymbol{\Xi}}_g \boldsymbol{\Lambda}_g^{(1)} \mathbf{M}_g^H \\ &\quad - \mathbf{M}_g \boldsymbol{\Lambda}_g^{(1)} \overline{\boldsymbol{\Xi}}_g^H \boldsymbol{\Gamma}_g + \mathbf{M}_g \boldsymbol{\Lambda}_g^{(1)} \mathbf{M}_g^H\Big) \\ &= Q^{-1}\text{Trace}\Big(\boldsymbol{\Gamma}_g^H \boldsymbol{\Sigma} \boldsymbol{\Gamma}_g - \mathbf{M}_g \boldsymbol{\Lambda}_g^{(1)} \mathbf{M}_g^H\Big).\end{aligned} \tag{16}$$

Since perfect random interleaving at each user is assumed, the covariance matrices $\boldsymbol{\Lambda}_g^{(i)}$, $i = 1, 2$ in (14) and (15) are diagonal. More precisely, they are given by

$$\begin{aligned}\boldsymbol{\Lambda}_g^{(1)} &= \hat{\boldsymbol{\Lambda}}_g \otimes \mathbf{I}_Q, \\ \boldsymbol{\Lambda}_g^{(2)} &= \text{ddiag}\big\{\boldsymbol{\Lambda}_1^{(1)}, ..., \boldsymbol{\Lambda}_{g-1}^{(1)}, \boldsymbol{\Lambda}_{g+1}^{(1)} ..., \boldsymbol{\Lambda}_G^{(1)}\big\}\end{aligned}$$

with $\hat{\boldsymbol{\Lambda}}_g \equiv \text{diag}\big\{1 - \varphi_{a_1}, ..., 1 - \varphi_{a_u}, ..., 1 - \varphi_{a_U}\big\}$, $a_u \in \mathcal{A}_g$ being the matrix containing the power levels of the soft-symbol estimates $\varphi_{a_u} \equiv \mathbb{E}[b_{q,a_u}^2(k)]$. The power levels may simply be estimated by the sample average over a complete frame of BPSK symbol estimates $\bar{b}_{q,n}(k)$ [25]. With the MSE (16) as our cost function, the *groupwise* MMSE filtering problem satisfying design criterion 3.2 can be expressed as

$$\begin{aligned}\tilde{\boldsymbol{\Gamma}}_g = \arg \min_{\boldsymbol{\Gamma}_g \in \mathbb{C}^{UQ \times MQ}} & Q^{-1}\text{Trace}\Big(\boldsymbol{\Gamma}_g^H \boldsymbol{\Sigma} \boldsymbol{\Gamma}_g - \mathbf{M}_g \boldsymbol{\Lambda}_g^{(1)} \mathbf{M}_g^H\Big) \\ \text{s.t. } & \text{diag}\{\mathbf{M}_g\} = \mathbf{1}_{UQ},\end{aligned} \tag{17}$$

where the constraint on matrix $\mathbf{M}_g$ is imposed to avoid the trivial solution $\tilde{\boldsymbol{\Gamma}}_g = \mathbf{0}$. To express (17) in a more convenient form, we define by $\hat{\boldsymbol{\Gamma}}_g \equiv \boldsymbol{\Gamma}_g(\mathbf{I}_U \otimes \mathbf{1}_Q) \in \mathbb{C}^{U \times QM}$ and $\boldsymbol{\Upsilon}_g \equiv \overline{\boldsymbol{\Xi}}_g(\mathbf{I}_U \otimes \mathbf{1}_Q) \in \mathbb{C}^{U \times QM}$ the subgroup's filtering and channel matrix, respectively. Using these notations, the MSE in (16) can be written as

$$\begin{aligned}\text{MSE}_g &= Q^{-1}\text{Trace}\Big(\boldsymbol{\Gamma}_g^H \boldsymbol{\Sigma} \boldsymbol{\Gamma}_g - (\mathbf{U}_g \otimes \mathbf{I}_Q)(\hat{\boldsymbol{\Lambda}}_g \otimes \mathbf{I}_Q) \\ &\quad \times (\mathbf{U}_g^H \otimes \mathbf{I}_Q)\Big) \\ &= Q^{-1}\text{Trace}\Big(\hat{\boldsymbol{\Gamma}}_g^H \boldsymbol{\Sigma} \hat{\boldsymbol{\Gamma}}_g - Q \mathbf{U}_g \hat{\boldsymbol{\Lambda}}_g \mathbf{U}_g^H\Big) \\ &= Q^{-1}\text{Trace}\Big(\hat{\boldsymbol{\Gamma}}_g^H \boldsymbol{\Sigma} \hat{\boldsymbol{\Gamma}}_g - Q^{-1} \hat{\boldsymbol{\Gamma}}_g^H \boldsymbol{\Upsilon}_g \hat{\boldsymbol{\Lambda}}_g \boldsymbol{\Upsilon}_g^H \hat{\boldsymbol{\Gamma}}_g\Big) \\ &= Q^{-1}\text{Trace}\Big(\hat{\boldsymbol{\Gamma}}_g^H \boldsymbol{\Sigma}_0 \hat{\boldsymbol{\Gamma}}_g\Big),\end{aligned} \tag{18}$$

where $\boldsymbol{\Sigma}_0 \equiv \boldsymbol{\Sigma} - Q^{-1} \boldsymbol{\Upsilon}_g \hat{\boldsymbol{\Lambda}}_g \boldsymbol{\Upsilon}_g^H$. Based on (18), we can rewrite the optimization problem (17) as

$$\begin{aligned}\breve{\boldsymbol{\Gamma}}_g \equiv \arg \min_{\hat{\boldsymbol{\Gamma}}_g \in \mathbb{C}^{U \times MQ}} & Q^{-1}\text{Trace}\big(\hat{\boldsymbol{\Gamma}}_g^H \boldsymbol{\Sigma}_0 \hat{\boldsymbol{\Gamma}}_g\big) \\ \text{s.t. } & Q^{-1}\text{diag}(\hat{\boldsymbol{\Gamma}}_g \boldsymbol{\Upsilon}_g^H) = \mathbf{1}_U.\end{aligned} \tag{19}$$

In Appendix A, it is shown that $\breve{\boldsymbol{\Gamma}}_g$ under the constraint in (19) can be derived as

$$\breve{\boldsymbol{\Gamma}}_g = \boldsymbol{\Sigma}^{-1} \boldsymbol{\Upsilon}_g \boldsymbol{\Theta}_g^{-1} \boldsymbol{\Omega}_g^{-1}, \tag{20}$$

where

$$\begin{aligned}\boldsymbol{\Omega}_g &\equiv Q^{-1}\text{ddiag}\big\{\boldsymbol{\Upsilon}_g^H \boldsymbol{\Sigma}^{-1} \boldsymbol{\Upsilon}_g \boldsymbol{\Theta}_g^{-1}\big\}, \\ \boldsymbol{\Theta}_g &\equiv \mathbf{I}_U - Q^{-1} \hat{\boldsymbol{\Lambda}}_g \boldsymbol{\Upsilon}_g^H \boldsymbol{\Sigma}^{-1} \boldsymbol{\Upsilon}_g.\end{aligned}$$

Rewriting (20) in the diagonal-block form (11), the optimal *groupwise* frequency domain MMSE filter $\tilde{\boldsymbol{\Gamma}}_g$ is obtained as

$$\tilde{\boldsymbol{\Gamma}}_g = \boldsymbol{\Sigma}^{-1} \overline{\boldsymbol{\Xi}}_g \big(\boldsymbol{\Theta}_g^{-1} \boldsymbol{\Omega}_g^{-1} \otimes \mathbf{I}_Q\big). \tag{21}$$

From (21), we observe that the filter computation requires the calculation of the inverse of the covariance matrix $\boldsymbol{\Sigma} \in \mathbb{C}^{QM \times QM}$. However, taking into account the block-diagonal structure of the frequency domain channel matrices $\overline{\boldsymbol{\Xi}}_g$ and $\overline{\overline{\boldsymbol{\Xi}}}_g$ and the symbol covariance matrices $\boldsymbol{\Lambda}_g^{(1)}$ and $\boldsymbol{\Lambda}_g^{(2)}$, we find that $\boldsymbol{\Sigma}$ is block-diagonal, and therefore its inverse can be efficiently computed, for example by using the LU-decomposition [30], with only $O(QM^3)$ operations per turbo iteration.

Lemma 3.3: *By setting $U = 1$, the proposed hybrid equalizer is equivalent to the conventional biased SC-MMSE FDE.*

For the special case of $U = 1$, i.e., the gth set $\mathcal{A}_g$ contains only the index of one user, Eqn. (21) reduces to the *unbiased* frequency domain MMSE filter

$$\tilde{\boldsymbol{\Gamma}}_g = \frac{\boldsymbol{\Sigma}^{-1} \overline{\boldsymbol{\Xi}}_g}{Q^{-1}\text{Trace}(\overline{\boldsymbol{\Xi}}_g^H \boldsymbol{\Sigma}^{-1} \overline{\boldsymbol{\Xi}}_g)}. \tag{22}$$

It can easily be shown that the resulting equalizer structure based on (22) and the conventional *biased* SC-MMSE FDE [10]-[12] have an identical LLR decision metric. Therefore, both schemes have equal performance in terms of BER.

Using (21) and (9), we may finally express the *groupwise* time-domain filter output at the equalizer as

$$\mathbf{z}_g(k) = \tilde{\mathbf{M}}_g \mathbf{c}_g(k) + \mathbf{v}_g(k), \tag{23}$$

where $\tilde{\mathbf{M}}_g = \breve{\mathbf{U}}_g \otimes \mathbf{I}_Q$ with $\breve{\mathbf{U}}_g = Q^{-1}\breve{\mathbf{\Gamma}}_g^H \mathbf{\Upsilon}_g$, and $\mathbf{v}_g(k)$ is the residual interference plus noise term.

B. Derivation of LLR

After groupwise filtering of the received signals, joint detection of the users' signals within one subgroup is performed. The symbol estimates corresponding to the users' signals of the gth subgroup to be jointly detected are first grouped together into vectors $\mathbf{z}_{g,q}(k) \equiv [z_{q,a_1}(k), ..., z_{q,a_u}(k), ..., z_{q,a_U}(k)]^T \in \mathbb{C}^{U\times 1}$, $a_u \in \mathcal{A}_g$, for all $q = 1, ..., Q$. These vectors are given by

$$\begin{aligned}\mathbf{z}_{g,q}(k) &= \mathbf{S}_q \mathbf{z}_g(k) \\ &= \breve{\mathbf{U}}_g \mathbf{c}_{g,q}(k) + \mathbf{v}_{g,q}(k),\end{aligned} \tag{24}$$

where $\mathbf{c}_{g,q}(k) = \mathbf{S}_q \mathbf{c}_g(k)$ and $\mathbf{v}_{g,q}(k) = \mathbf{S}_q \mathbf{v}_g(k)$ are the gth subgroup's transmitted signal vector and the residual interference and noise vector during the qth transmission period, respectively, obtained from $\mathbf{c}_g(k)$ and $\mathbf{v}_g(k)$ by multiplication with selection matrix $\mathbf{S}_q \equiv \mathbf{I}_U \otimes \mathbf{e}_q^T$. The equivalent channel matrix $\breve{\mathbf{U}}_g$ in (24) is found with (20) as

$$\breve{\mathbf{U}}_g = \mathbf{\Omega}_g^{-1} \mathbf{\Theta}_g^{-1} \mathbf{\Upsilon}_g^H \mathbf{\Sigma}^{-1} \mathbf{\Upsilon}_g.$$

In order to compute LLR messages for the filtered signal components $\mathbf{z}_{g,q}(k)$ in (24), we resort to the Gaussian approximation (see, e.g., [4], [7]) of the residual interference plus noise term at the filter output, that is known to be valid in the large system case. Consequently, the vector $\mathbf{v}_{g,q}(k)$ can be modeled as a multivariate circularly symmetric Gaussian random process with zero-mean and covariance matrix

$$\begin{aligned}\mathbf{R}_g &= \mathbb{E}[\mathbf{v}_{g,q}(k)\mathbf{v}_{g,q}^H(k)] \\ &= Q^{-1}\mathbf{\Omega}_g^{-1}\mathbf{\Theta}_g^{-1}\mathbf{\Upsilon}_g^H\mathbf{\Sigma}^{-1}\mathbf{\Upsilon}_g\mathbf{\Omega}_g^{-1}.\end{aligned} \tag{25}$$

We remark that $\breve{\mathbf{U}}_g$ and $\mathbf{R}_g$ are identical for all (q, k) and have to be computed only once for each subgroup and turbo iteration. Therefore, the *extrinsic* LLR for each $b_{q,a_u}(k)$ is obtained as [25]

$$\lambda_e[b_{q,a_u}(k)] = \log \frac{\sum\limits_{\mathbf{x}\in\mathcal{X}_u^{<+1>}} \exp\left[\rho_{g,q}(k) + \sum\limits_{\forall j: j\neq u, x(j)=+1} \zeta_e[b_{q,a_j}(k)]\right]}{\sum\limits_{\mathbf{x}\in\mathcal{X}_u^{<-1>}} \exp\left[\rho_{g,q}(k) + \sum\limits_{\forall j: j\neq u, x(j)=+1} \zeta_e[b_{q,a_j}(k)]\right]}, \tag{26}$$

where $\rho_{g,q}(k)$ is the MAP-decision metric defined as

$$\rho_{g,q}(k) \equiv -\big(\mathbf{z}_{g,q}(k) - \breve{\mathbf{U}}_g\mathbf{x}\big)^H \mathbf{R}_g^{-1}\big(\mathbf{z}_{g,q}(k) - \breve{\mathbf{U}}_g\mathbf{x}\big), \tag{27}$$

TABLE I
NUMBER OF COMPLEX MULTIPLICATIONS PER RECEIVED SYMBOL PER ITERATION.

	Complex Multiplications
Groupwise FDE	$GMU(2M+2U+1) + 2/3(GU^3+M^3)$ $+6GU^2 + 5M^2 + 1/3(UG+M) + 6G + 4$
FFT/IFFT Operations	$(M(N+1)+2N)\log_2 Q$
Group Detection	$G2^U + GU(2U+1) + G$

and $\mathcal{X}_u^{<\pm 1>}$ is the set of 2^U BPSK data symbols $\mathbf{x} \in \mathcal{X}_u^{<\pm 1>}$ for which the uth component $x_u = \pm 1$.

An approximate operation count in terms of complex multiplications required by the proposed hybrid FDE per turbo iteration is shown in Table I. The algorithm needs $M(N+1)+2N$ Q-point DFT/IDFT-operations per transmitted block, which is due to the frequency domain conversion of the received signal, the soft feedback from channel decoding and the channel estimates. The calculation of the soft estimates requiring the $tanh(\cdot)$ function is not taken into account. Observing Table I, we find that the overall complexity for the case of $M \geq N$ is of order $O\big(G2^U + M(M^2 + N\log_2 Q)\big)$. We remark that when the number of users per subgroup is high, i.e., for large values of U, the exact calculation of (26) becomes computational expensive. In such cases, the complexity can be reduced by applying list soft-output sphere detection [27].

C. Comparison with other Criteria

Different alternative choices of optimization criteria can be used for cancellation of interference components between subgroups. In [17], equalization is performed by linear filtering minimizing the unconditional MSE

$$\text{minimize } Q^{-1}\mathbb{E}\left[\left\|\mathbf{P}_g\Big(\mathbf{r}(k) - \overline{\overline{\mathbf{H}}}_g \bar{\mathbf{d}}_g(k)\Big) - \mathbf{c}_g(k)\right\|^2\right], \tag{28}$$

where $\mathbf{P}_g \in \mathbb{C}^{QU\times QM}$ is the time domain MMSE block-filtering matrix. Also, as shown in [17], a frequency domain equivalent can be derived from $\mathbf{P}_g$ by utilizing the eigenvalue decomposition of the circulant channel matrices. We note that the criterion in (28) in the absence of *a priori* information is simply a block-wise notation of the symbol-wise (unconditional) MSE formulation from [5]. The SC-MMSE filtering block resulting from (28) is therefore during the first turbo iteration equivalent to the standard SC-MMSE filtering that removes interference *user-by-user* from the received signal to separate the transmitted signals. Unlike to the above MSE criterion, the objective of our criterion (17) is to obtain a frequency domain *groupwise* MMSE filter that *jointly* suppresses residual interferences for the users' signals in each subgroup. Besides, more important, only the MSE in (13) can be used to evaluate the performance of each subgroup, which is needed for adaptive user grouping incorporating *a priori* information from channel decoding, as considered in Section IV.

Recently, the authors of [22] proposed a *groupwise* filtering technique maximizing the SINR in each subgroup for *non-iterative* joint detection of multi-antenna signals in flat-fading MIMO channels. Here, we extend the approach from [22]

to iterative frequency domain soft interference cancellation equalization employing *groupwise* maximum-SINR filtering. Suppose again that design criterion 3.1 holds. Then, using the notations in (3)-(9), the filtering matrix maximizing the SINR for the gth subgroup can be obtained as

$$\check{\mathbf{\Gamma}}_g \equiv \arg \max_{\{\hat{\mathbf{\Gamma}}_g \in \mathbb{C}^{UQ \times MQ}\}} \text{SINR}_g, \tag{29}$$

where SINR_g is defined as

$$\text{SINR}_g \equiv \frac{\mathbb{E}\big[\, \|\mathbf{M}_g \mathbf{c}_g(k)\|^2 \,\big]}{\mathbb{E}\big[\, \|\mathbf{z}_g(k) - \mathbf{M}_g \mathbf{c}_g(k)\|^2 \,\big]}.$$

As shown in Appendix B, the optimal value of $\check{\mathbf{\Gamma}}_g$ can be found as a solution of a generalized eigenvalue problem.

We now present a theorem that compares the proposed MSE and SINR criteria.

Theorem 3.4: *The groupwise hybrid equalizers based on MSE and SINR criteria in (17) and (29), respectively, have an identical MAP decision metric.*

Proof: The proof is given in Appendix C. ∎

The *groupwise* MMSE and SINR-based filter designs in (17) and (29), respectively, thus lead to turbo equalizer structures having identical complexities and *extrinsic* output LLRs.

IV. Group Selection Methods

The performance of the proposed turbo equalizer is largely determined by the assignment of the users' signals to subgroups. In [22], a GS method based on a capacity criterion was proposed that maximizes the achievable information rate of MIMO systems employing *non-iterative* group detection. The same authors presented in [31] a grouping scheme using a $\min$-$\max$ subgroup SINR formulation. The algorithms in [22] and [31] compute the GS metric for all possible group partitions, and then select the optimum one. Since calculating the GS metric for each partition involves a number of complex matrix calculations, these schemes are restricted to systems having a small number of users or groupings which generate large subgroups. Other GS methods exploiting the channel correlation matrix $\mathbf{S}$ have been presented in [21] and [16]. The algorithm in [21] optimizes the grouping for each individual antenna of the MIMO system by allowing overlapping subgroups. Although such an antenna-by-antenna optimized scheme maximizes performance, it requires very high complexity cost in practical system configurations. The GS approach from [16] reduces complexity by adopting only $\max/\min$ operations to successively form *disjoint* subgroups maximizing the pairwise correlation sum.

In this section, several new GS criteria for *iterative groupwise* MMSE equalization are proposed. Particularly, an algorithm is presented that computes an MSE criterion using the available *a priori* knowledge about the code bits to find, among all possible combinations of G subgroups, the group partition guaranteeing optimum performance at each turbo iteration. Also, different schemes providing a static grouping valid for all turbo iterations are discussed. In this regard, a very simple channel correlation-based algorithm is proposed which does not need $\max/\min$ or compare operations. The performance of these methods will be compared in Section VI.

A. Grouping based on Min-Max-MSE

First, we propose a GS criterion based on minimization of the MSE at the *groupwise* filter output. The MSE for the gth subgroup is obtained by substituting (20) into (16), which results in the following expression:

$$\text{MSE}_g = \text{Trace}(\mathbf{\Omega}_g^{-1}). \tag{30}$$

The overall performance of the proposed FDE is mainly dominated by the subgroup, whose MSE is the highest among all subgroups. In order to maximize performance, we select among all possible group partitions the one that minimizes the worst subgroup's MSE. A convenient criterion for grouping N users into G subgroups is therefore given by

$$\hat{p} = \arg \min_{1 \le s \le S} \max_{1 \le g \le G} \text{Trace}(\mathbf{\Omega}_g^{(s)-1}), \tag{31}$$

where S denotes the total number of possible combinations of pairs, and $\text{Trace}(\mathbf{\Omega}_g^{(s)-1})$ is the MSE of the gth subgroup corresponding to the sth ($1 \le s \le S$) combination. Based on (31), we devise a simple method, which is summarized in Algorithm 1, that dynamically forms G subgroups at each turbo iteration.

Algorithm 1 Dynamic MSE-based grouping

1: Calculate at each turbo iteration the MSE in (30) for all subgroups and possible pairings.
2: Solve (31).

Algorithm 1 requires the calculation of $T = \binom{N}{U}$ inverses of $U \times U$ matrices and it needs to perform the minimum operation $S = \binom{N}{U}\binom{N-U}{U} \cdots \binom{U}{U} / (G \cdot (G-1) \cdot \ldots \cdot 2)$ times. This leads to a high complexity if the numbers of users or subgroups are large. For example, for $N = 16$ and $G = 4$, we obtain $T = 1820$ and $S = 2627625$. To reduce complexity, instead of dynamically forming the subgroups at each turbo iteration, a static set can be used for all turbo iterations. This is the motivation behind the second grouping method, which is summarized in Algorithm 2, that performs the allocation in (31) only once at the first turbo iteration.

Algorithm 2 Static MSE-based grouping

1: Calculate at the first turbo iteration the MSE in (30) for all subgroups and possible pairings.
2: Solve (31).

The MSE in (30) could also be replaced by the subgroup SINR (47). However, calculating the SINR requires for each possible partition the Cholesky factorization and the eigenvalue decomposition of the large $QM \times QM$ matrices (44) and (45), respectively, which may be impractical for large DFT-sizes and number of receive antennas.

B. Grouping based on Correlation

Next, we propose a correlation-based method to assign users into subgroups. For this purpose, let us define by

$$\rho_{k,l} = \frac{\text{Trace}\big(\mathbf{\Xi}_k^H \mathbf{\Xi}_l\big)}{\sqrt{\text{Trace}\big(\mathbf{\Xi}_k \mathbf{\Xi}_k^H\big)} \cdot \sqrt{\text{Trace}\big(\mathbf{\Xi}_l \mathbf{\Xi}_l^H\big)}}$$

the pairwise normalized correlation coefficient between user channel k and l. Further, let $\mathbf{V}$ be the upper triangular correlation matrix with entries

$$[\mathbf{V}]_{k,l} = \begin{cases} \rho_{k,l}, k > l \\ 0, \text{ otherwise.} \end{cases}$$

At high SNR, the performance of the equalizer is largely influenced by the minimum euclidean distance between the users' channels of the G subgroups. It is therefore desirable to find a group partition that minimizes the maximum pairwise channel correlation between members of different subgroups. Given the normalized correlation matrix $\mathbf{V}$, this problem can formally be expressed as

$$\min \max_{k\in\mathcal{A}_{g_1}, l\in\mathcal{A}_{g_2}, g_1\neq g_2, 1\leq g_1, g_2\leq G} \rho_{k,l}. \quad (32)$$

Solving (32) is a combinatorial problem that requires an exhaustive search over all possible partitions. Obviously, this is prohibitively expensive in terms of complexity for large N and G. Instead, we propose a greedy approach, which yields a suboptimal solution, but reduces drastically the computational load. The proposed method is listed in Algorithm 3.

Algorithm 3 Static correlation-based grouping

1: Initialize the subgroup sets $\mathcal{A}_n = \{n\}$, $n = 1, ..., N$.
2: Initialize the set containing the user indexes $\mathcal{N} = \{1, ..., N\}$.
3: Sort the normalized cross-correlation values of matrix $\mathbf{V}$ in descending order in a vector $\mathbf{v}$, and keep the information of the user indexes i, j in $\mathbf{V}$.
4: Set $l = 1$.
5: **if** $|\mathcal{N}| > G$ **then**
6: Select the lth position in vector $\mathbf{v}$. Let i, j be the corresponding indexes to that position.
7: **if** $i \in \mathcal{A}_{n_1}$ and $j \in \mathcal{A}_{n_2}$, $n_1 \neq n_2$, $n_1, n_2 \in \mathcal{N}$ **then**
8: **if** $|\mathcal{A}_{n_1}| + |\mathcal{A}_{n_2}| \leq U$ **then**
9: $\mathcal{A}_{n_1} = \mathcal{A}_{n_1} \cup \mathcal{A}_{n_2}$
10: Remove index n_2 from set $\mathcal{N}$.
11: **end if**
12: **end if**
13: **end if**
14: Increment l, and repeat step 5 until the last element of vector $\mathbf{v}$, or if G subgroups are filled, i.e., $|\mathcal{N}| = G$.

Algorithm 3 first allocates the N users into N subgroups, and sorts the correlation values of matrix $\mathbf{V}$ in descending order in a vector $\mathbf{v}$. The algorithm then iteratively allocates two users corresponding to the lth position (iteration index l) of vector $\mathbf{v}$ into one subgroup (lines 5-13). At each iteration, the two groups having the maximum pairwise channel correlation are merged. As a result, highly spatially correlated users are allocated to the same subgroup. This selection may not be optimal with respect to (32), however, it reduces the noise enhancement due to the MMSE interference suppression of highly correlated user signals. The advantage of the preceding algorithm over the other two methods is that search complexity is significantly reduced and computation of matrix inverses is not required.

V. Convergence Analysis

The convergence property of the *groupwise* FDE is analyzed using correlation charts [13], [18]. The correlation chart relies, similar to the well known extrinsic information transfer (EXIT) chart [26], on the assumption that all LLR messages of the equalizer and the channel decoders can be modeled as discrete-time ergodic processes that satisfy the *exponential symmetry condition*, such that $p(x) = p(-x)\exp(x)$, where $p(x)$ is the probability density function of an LLR message.

Let $\varphi_{(\cdot,n)} \equiv \mathbb{E}[x_n e_n]$ be the correlation between the true binary transmit signal x_n and its estimate $e_n \equiv \mathbb{E}\big[x_n \,\big|\lambda_{(\cdot)}[x_n]\,\big] = \tanh\big((1/2)\lambda_{(\cdot)}[x_n]\big)$, given the *extrinsic* LLR $\lambda_{(\cdot)}[x_n]$ of user n, where the variable x_n is a placeholder for the binary signals $a_n(i)$ or $b_{q,n}(k)$. Similarly, we define $\alpha_{(\cdot,n)} \equiv \mathbb{E}\big[x_n \tanh\big((1/2)\zeta_{(\cdot)}[x_n]\big)\big]$ as the correlation between the true binary signal x_n and its estimate $\tanh\big((1/2)\zeta_{(\cdot)}[x_n]\big)$, given the *a priori* LLR $\zeta_{(\cdot)}[x_n]$. Moreover, following [26], we assume that the conditional probability density functions of the random variables $(1/2)x_n\zeta_{(\cdot)}[x_n]$ can be well approximated by Gaussian distributions, i.e., $(1/2)x_n\zeta_{(\cdot)}[x_n] \sim \mathcal{N}(\mu_x, \sigma_x^2)$, where due to the *exponential symmetry* property of the LLRs, $\mu_x/\sigma_x^2 = 1$. Under these assumptions, the convergence behavior of the FDE can be described by a set of N correlation functions,

$$\varphi_{e,n} \equiv f_{e,n}(\alpha_{e,1}, ..., \alpha_{e,n}, ..., \alpha_{e,N}) \in [0,1], \quad \alpha_{e,n} \in [0,1], n = 1, ..., N, \quad (33)$$

where $\varphi_{e,n}$ and $\alpha_{e,n}$ denote the correlation at the output and input of the equalizer, respectively, corresponding to the nth user. These functions are determined by Monte-Carlo simulations, where the correlation values at the equalizer output are calculated, by invoking the ergodicity, as

$$\varphi_{e,n} \approx \frac{1}{QK}\sum_{q=0}^{Q-1}\sum_{k=1}^{K-1} b_{q,n}(k)\tanh\big((1/2)\lambda_e[b_{q,n}(k)]\big), \forall n.$$

Note that each equalizer function $f_{e,n}(\cdot)$ is conditioned on the specific channel realization and receiver noise power.

Similar, we describe the correlation function for each SCCC decoder that combines the operation of the inner and outer decoder into a single decoder component as [19]

$$\varphi_{d,n} \equiv f_{d,n}(\alpha_{d,n}), n = 1, ..., N.$$

The function $f_{d,n}(\cdot)$ can be used to obtain as estimate of BER after channel decoding at each turbo iteration of the turbo equalizer [13].

As indicated by (33), each equalizer correlation function depends on N input values and the corresponding surface is $(N+1)$-dimensional. The convergence behavior of the iterative receiver is described by several interconnected multi-dimensional correlation charts. In order to avoid such a cumbersome visualization, we use the projection technique from [29] to reduce the dimensionality of each equalizer correlation surface to two dimensions (2D). We define $g_{e,n}(\alpha_{e,n})$, $n = 1, ..., N$ as the projected equalizer correlation function corresponding to the nth user. This function may be written

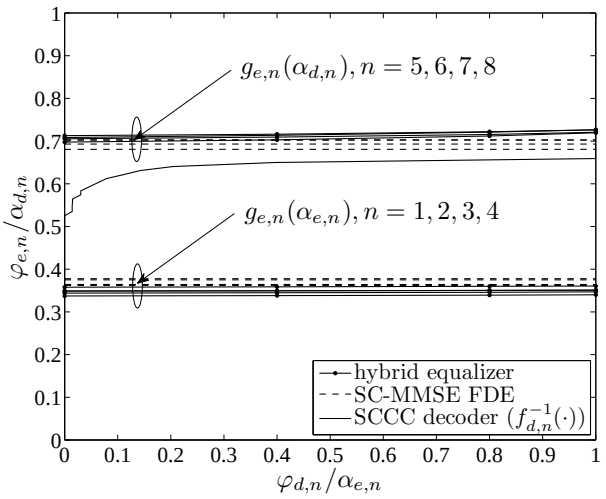

Fig. 1. Correlation functions (projection) of the proposed hybrid equalizer ($U = 4$) and the standard SC-MMSE FDE ($U = 1$) for each user for a single random channel realization at $E_s/N_0 = 2$ dB. $Q = 512$.

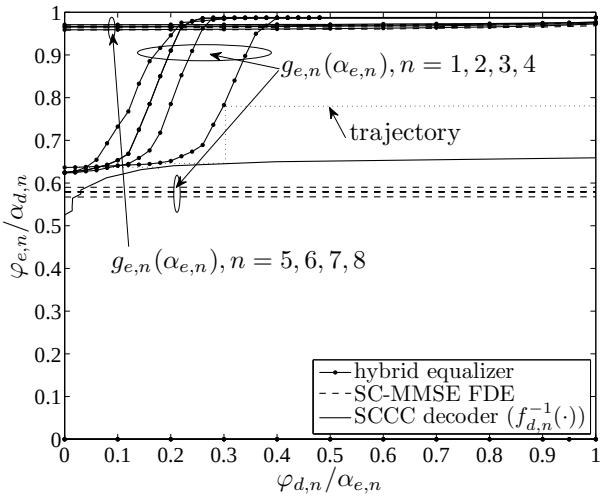

Fig. 2. Correlation functions (projection) of the proposed hybrid equalizer ($U = 4$) and the standard SC-MMSE FDE ($U = 1$) for each user for a single random channel realization at $E_s/N_0 = 6$ dB. $Q = 512$.

as

$$g_{e,n}(\alpha_{e,n}) \equiv \lim_{T_e \to \infty} f_{e,n}(\varphi_{d,1}^{(T_e)}, ..., \varphi_{d,n-1}^{(T_e)}, \alpha_{e,n}, \varphi_{d,n+1}^{(T_e)}, ..., \varphi_{e,N}^{(T_e)}), \alpha_{e,n} \in [0,1], \forall n, \quad (34)$$

where for each index n, the $N-1$ equalizer's input correlations $\varphi_{d,r}^{(T_e)}$, $r = 1, ..., N$, $r \neq n$ are the result of the following recursions:

$$\varphi_{e,r}^{(l)} = f_{e,r}(\varphi_{d,1}^{(l)}, ..., \varphi_{d,n-1}^{(l)}, \alpha_{e,n}, \varphi_{d,n+1}^{(l)}, ..., \varphi_{d,n}^{(l)}) \forall r,$$
$$\varphi_{d,n}^{(l+1)} = f_{d,n}(\varphi_{e,n}^{(l)}), \forall n, \text{ for } l = 0, ..., T_e \text{ with } \varphi_{d,n}^{(0)} = 0, \forall n. \quad (35)$$

Using the above 2D-projections, the convergence behavior can now be analyzed by N independent 2D-correlation charts, one for each user.

Fig. 1 and 2 illustrate the projected correlation curves of the *grouwpise* equalizer and the conventional SC-MMSE FDE for a single random channel realization at SNR $E_s/N_0 = 2$ dB and $E_s/N_0 = 6$ dB, respectively. The correlation functions of the SCCC decoders are identical for all users and obtained when the outer encoder is a rate-$1/2$, memory-4, recursive convolutional code defined by the generator $(g_r, g_0) = (23, 35)$, where g_r denotes the feedback polynomial, and the inner encoder is a simple rate-1 code having the polynomials $(g_r, g_0) = (3, 2)$. An $N = 8$ multiuser scenario is assumed where four of the eight users' channels are highly spatially correlated at the transmit side and the remaining users' channels are close to orthogonal. The off-diagonal elements of the correlation matrix $\mathbf{S}$ are set to $[\mathbf{S}]_{ij} = 0.9$, for $1 \leq i, j \leq 4$, $i \neq j$, and $[\mathbf{S}]_{ij} = 0$ otherwise. The number of subgroups of the *groupwise* FDE is set to $G = 2$ and the four highly correlated users' signals are allocated into one subgroup.

Fig. 2 also shows exemplary the trajectory, representing the correlation exchange between the equalizer and the SCCC channel decoder, corresponding to the first user. A vertical step between the 2D-projected equalizer curve and the SCCC decoder curve corresponds with respect to (35) to a large number of iterations between the equalizer and all SCCC channel decoders (except the first one), until the equalizer output correlation $\varphi_{e,1}^{(l)}$ has converged to a fixed value. A horizontal step between both curves represents a single activation of the SCCC channel decoder of the first user.

As observed from Fig. 1, for the low SNR value of 2 dB, both turbo equalizers have similar performances for all users. Moreover, we find that only for the users' signals having low spatial correlation the convergence tunnels between the equalizer and decoder curves are existent and convergence of turbo equalization may be achieved. For the remaining highly correlated users' signals the two turbo equalizers fail to convergence and thus to decode these users' messages. In contrast, as shown in Fig. 2, when increasing the SNR value to 6 dB, we observe that only the *groupwise* FDE is able to form an open convergence tunnel for the four highly spatially correlated user signals and thus to successfully decode all users' messages. This indicates that *groupwise* equalization improves the convergence threshold and can achieve better performance than standard SC-MMSE FDE in the presence of high spatial channel correlation.

VI. Numerical Results

In this section, numerical results of BER and frame error rate (FER) simulations conducted to evaluate the performance enhancement achieved by the proposed *groupwise* equalizer over the standard SC-MMSE FDE are presented. We consider a single carrier block transmission system with DFT-size $Q = 512$. Two different multiuser system setups having $N = M = 4$ and $N = M = 8$ users/receive antennas are investigated. The turbo equalizer performs $T_e = 10$ iterations between the equalizer and the N SCCC channel decoders. We assume a static activation schedule of the components of the receiver, where after each activation of the equalizer, decoding of all SCCC decoders proceeds iteratively over

TABLE II
SYSTEM PARAMETERS.

Tx antennas N	4/8
Rx antennas M	4/8
DFT length Q	512 symbols
Frame length KQ	4096 symbols
Outer Encoder	Rate-1/2, Memory-4 RSC code ([23, 35])
Inner Encoder	Rate-1 memory-1 RSC code ([3,2])
Stochastic Channel Model	Rayleigh block-fading MIMO channel (equal average power per tap) with Kronecker spatial correlation model
Channel Memory L	22/32
Interleaving	Random
Iterations	$T_e = 10$, $T_d = 10$
Channel estimation	Perfect

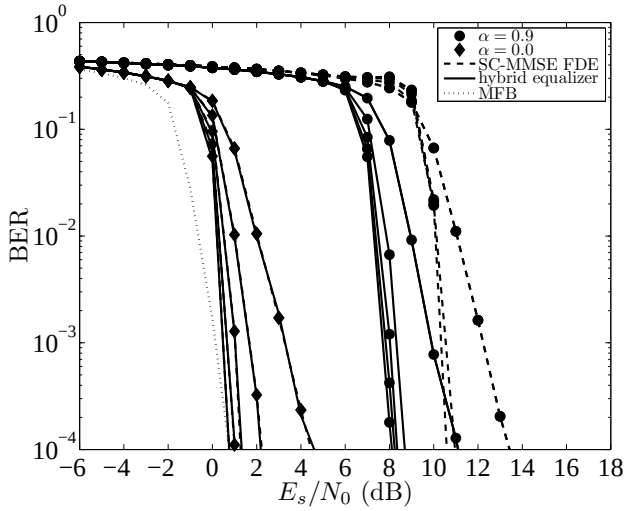

Fig. 3. Average BER performance of the proposed hybrid scheme and the standard SC-MMSE FDE at each turbo iteration of an $N = M = 4$ multiuser system for Rayleigh fading channels with spatial transmit correlation values $\alpha = 0.0$ and $\alpha = 0.9$.

$T_d = 10$ iterations between the inner and outer SCCC decoder. The numbers of iterations are chosen to be large enough to ensure convergence. Two channel models are considered in the simulations: first a simple $L = 32$-tap Rayleigh block-fading MIMO channel with uncorrelated receive antennas and equal average tap-energy and second an $L = 22$-tap measurement data-based MIMO channel. The channel gains are constant during the transmission of one frame of 4096 BPSK symbols per user, but change independently from frame to frame. Table II summarizes the major simulation parameters.

For the simulations, the average SNR at the receiver is defined as

$$\frac{E_s}{N_0} \equiv \frac{\sum_{n=1}^{N}\sum_{m=1}^{M}\sum_{l=0}^{L-1}\mathbb{E}\left[|h_{n,m}(l)|^2\right]E_0}{M\sigma_0^2},$$

where E_0 is the energy per symbol at the transmitter.

A. Stochastic Channel Model Based Results

Fig. 3 shows the BER performance for the $L = 32$-tap Rayleigh fading channel at each turbo iteration achieved by the two turbo equalizers for the $N = M = 4$ multiuser system in a scenario where all four users channels are identically spatially correlated with parameter $\alpha = 0.0$ or $\alpha = 0.9$. The correlation factor α corresponds to the off-diagonal elements of the transmit correlation matrix $\mathbf{S}$, i.e., $[\mathbf{S}]_{i,j} = \alpha$ for $1 \leq i, j \leq N$, $i \neq j$. The groupsize is set to $U = N$ ($G = 1$) such that all users are allocated into a single group. In this setup, all ISI components of the received signals from the M antennas are suppressed by *groupwise* MMSE filtering, while the separation of the users's transmitted signals is performed by MAP symbol detection. As a reference point, Fig. 3 also shows the simulation result of the corresponding matched filter bound (MFB) achieved when all interference has been removed in the system. The MFB serves as a lower bound on the BER of both turbo receivers here, obtained when the LLR feedback from the N channel decoders is perfect. According to Fig. 3, the two systems achieve identical performances at each turbo iteration and thus, they offer the same signal separation capabilities when the users' channels are spatially uncorrelated ($\alpha = 0.0$). Moreover, we find that the gap to the MFB vanishes at SNRs larger than 0.8 dB. In the presence of high spatial correlation ($\alpha = 0.9$), however, the simulation results indicate that the *groupwise* scheme outperforms the standard SC-MMSE FDE by 2.2 dB SNR at BER=10^{-4}.

Next, we consider the $N = M = 8$ multiuser scenario with $[\mathbf{S}]_{i,j} = \alpha$ for $1 \leq i, j \leq 4$, $i \neq j$ and $[\mathbf{S}]_{i,j} = 0$ for $5 \leq i, j \leq 8$, $i \neq j$. In this case, we chose a groupsize of $U = 4$ and allocate the four correlated user signals into the first subgroup. Fig 4 (a) and (b) depict the resulting BER and FER curves, respectively, for the two subgroups and turbo receivers of this system setup with the correlation value α as a parameter. As can be seen, the performance of users in the first subgroup significantly degrades for both turbo schemes with increasing values of α. Clearly, the larger the spatial correlation the larger the gain achieved by the *groupwise* scheme over the standard equalizer. Moreover, we see that for the correlated case ($\alpha = 0.9$), convergence of the *groupwise* FDE is initiated at an SNR of around 6 dB, which is consistent with the analysis in Section V. On the other hand, we observe that the performance of the second subgroup is nearly identical for all values of α, indicating that both turbo schemes can perfectly separate the signals between both subgroups.

More importantly, we observe that the slope of the FER curves remains identical when increasing the value of α, implying that the achievable diversity order is maintained, regardless of the users' spatial channel correlation. Similar to the results obtained in [28] for linear MMSE detectors, we notice that spatial channel correlation does not have any impact on the diversity order of MMSE-based turbo systems.

B. Channel-Sounding Data Based Evaluation and Results

In the previous subsection, the performance of the *groupwise* equalizer was analyzed utilizing a stochastic MIMO channel model with predefined fixed spatial correlations. In realistic scenarios, however, the spatial-temporal properties of the radio channel depend on the propagation environment and the location of the mobile users and the receiver. Since these channel properties are strongly time-varying, the spatial transmit and receive correlation matrices constructed from

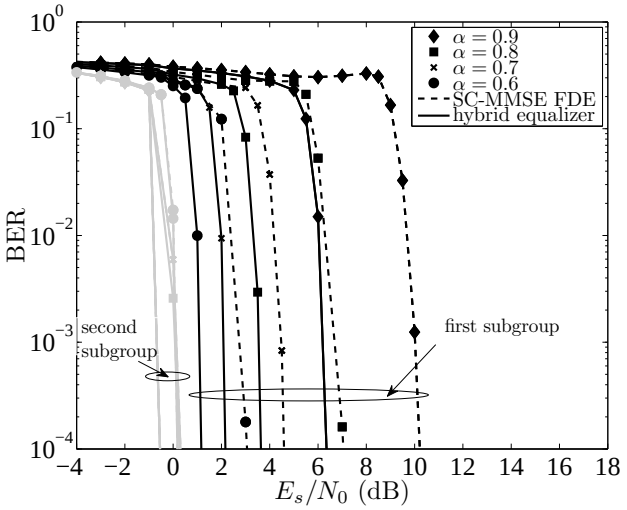

(a)

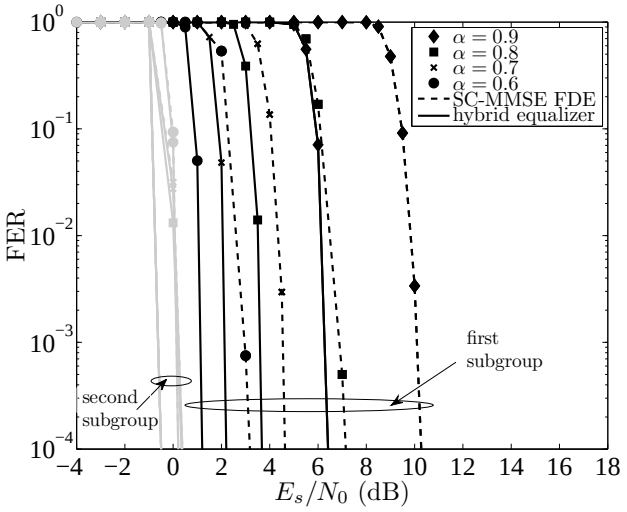

(b)

Fig. 4. Average BER and FER performance for the two subgroups (black: first subgroup (user 1 to 4)), gray: second subgroup (user 5 to 8)) of the hybrid scheme and the standard SC-MMSE FDE for an $N = M = 8$ multiuser system over Rayleigh fading channels with varying spatial transmit correlation values α.

the MIMO channel matrix [23], are time-varying as well. The two extreme cases leading to relatively high and low spatial correlation coefficients between the users' channels are, in general, the line-of-sight (LOS) and the non-line-of-sight (NLOS) propagation scenario, respectively.

In order to assess the practicality of the *groupwise* FDE in real fields, the performance is evaluated in this subsection by a series of simulations using channel-sounding field measurement data. For this purpose, a MIMO measurement campaign was conducted in the city center of Ilmenau, Germany. A top view of the considered urban micro-cell scenario is shown in Fig. 5. The measurement route has a length of approximately 60 m and was sampled with 2000 snapshots, corresponding to a distance of about 0.03 m between neighboring snapshots. An 16-element uniform circular array (UCA) with minimum element spacing of half the wavelength was used at the

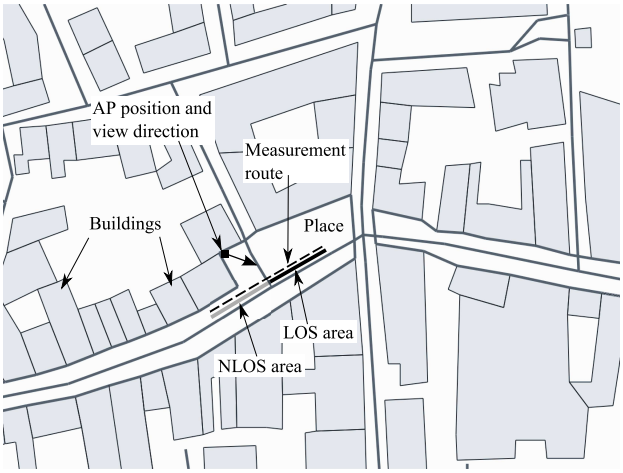

Fig. 5. Overview of measurement route and position of AP.

TABLE III
MEASUREMENT CAMPAIGN SETUP.

Scenario	Urban micro-cell
Environment	Open place with LOS cond. and pedestrain street with NLOS cond.
Track length	60 m
Channel Sounder	RUSK ATM, Medav GmbH
Transmit array	UCA, 16 elements
Receive array	ULA, 8 elements
Transmitter height/tilt	1.5 m/0°
Receiver height/tilt	4 m/2°-3° down
Transmit power	33 dBm at power amplifier output
Center frequency	5.2 GHz
Bandwidth	120 MHz
AGC switching	between MIMO snapshots
Maximal velocity	6 km/h

transmitter side as a mobile terminal (MT). The MT was moved at walking speed along the route marked by the dashed line shown in Fig. 5. At the receiver side, an 8-element uniform linear array (ULA) with element spacing of 0.4 times wavelength was used as an access point (AP). The receiver position was fixed and the height of the ULA was about 4 m above ground. The measurement route can roughly be divided into two regions; the first part in front of the large open place is mainly dominated by LOS propagation between MT and AP; the second part at half of the route, the MT moves from the open place into the pedestrian street, is mainly characterized by NLOS propagation. The area was surrounded by buildings with a height of approximately 10 to 15 m. In order to highlight the LOS and NLOS propagation conditions along the measurement route, the normalized total receive power at the AP is depicted in Fig. 6. The major specifications of the measurement campaign and the antenna setup are summarized in Table III.

1) Preprocessing of Channel-Sounding Data: The measured CIRs are preprocessed to be applicable in system simulations. Following [33], the noise power estimation and cut method is applied to each measured CIR to remove the influence of the measurement noise. Moreover, a subband of 20 MHz, corresponding to the channel bandwidth used in the system simulations, is extracted from the measurement data at the center frequency. The channel matrices for the multiuser

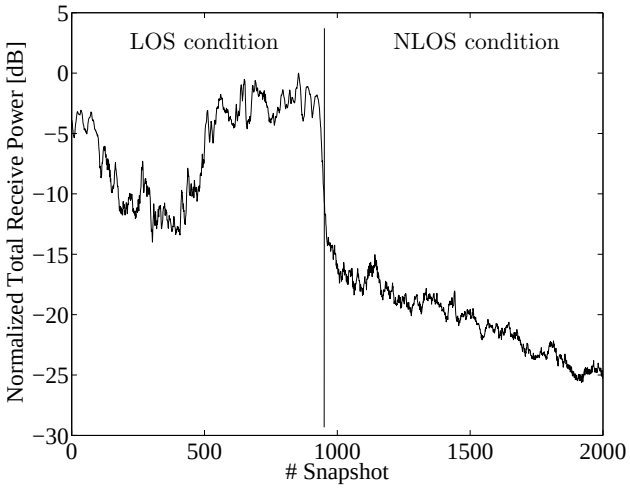

Fig. 6. Normalized total receive power along measurement route

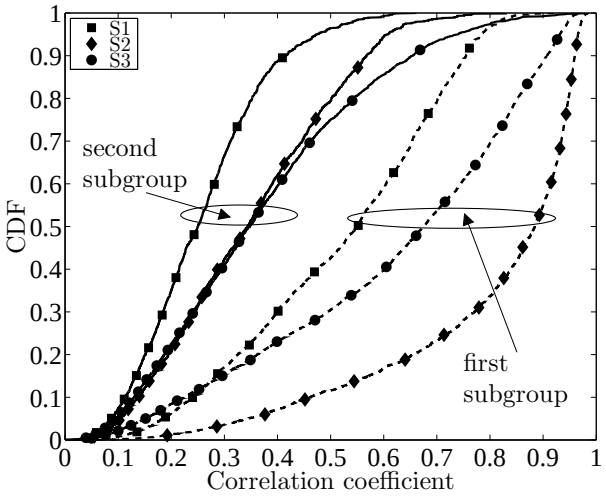

Fig. 7. CDF of pairwise users' channel correlation coefficient for each subgroup of the three multiuser scenarios.

setup are generated by combining the CIRs at eight randomly chosen mobile positions along the measurement route. At each position, one element of the antenna array at the transmitter side is randomly selected. This results in $N = M = 8$ MIMO channels. Three different multiuser scenarios are considered for system simulations.

S1) In the first scenario, the eight users are randomly distributed into two subgroups. The four users of the first and second subgroup are placed in the subarea with LOS and NLOS propagation condition, respectively. The two subgroups are well separated by 1000 snapshots, which corresponds to a distance of approximately 30 m between the MTs. Furthermore, the distance between users within each subgroup is fixed and set to 100 snapshots, resulting in a spatial separation of around 3 m. The two subgroups are moved along the measurement route until the end of the LOS/NLOS subarea is reached. This multiuser scenario reflects the behavior of moving, spatially, spacious, located users.

S2) The second multiuser scenario is identical to the first scenario, except that the spatial separation between the users in each subgroup is reduced to 5 snapshots (≈ 0.15 m). This scenario reflects the behavior of moving, spatially, very dense, located users.

S3) The third multiuser scenario models a random drop-based approach. Each drop is defined over 10 subsequent snapshots (≈ 0.30 m) by randomly allocating the eight users into two subgroups that are placed in the subareas with LOS/NLOS propagation condition. The radius of the two subgroups is fixed and set to 15 snapshots (≈ 0.45 m). Moreover, the users' positions within each subgroup and the subgroups' center positions on the measurement route are randomly chosen for each drop. Similar to the spatial channel modeling (SCM) or WINNER channel model [34], the drops are independent and represent randomly selected multiuser setups, where the MIMO channel undergoes fast fading according to the mobile movement of the users.

Fig. 7 shows the cumulative density function (CDF) of the pairwise users' channel correlation coefficient for the three multiuser scenarios S1, S2 and S3. In all three scenarios, as expected, we observe that users (from the first subgroup) placed in the LOS subarea experience higher spatial correlations than users (from the scond subgroup) placed in the NLOS subarea. Furthermore, we find that the largest correlation coefficients are obtained for the spatially, closely, located users from scenario S2.

Fig. 8 (a) and (b) depict the BER performance for the two subgroups achieved by the *groupwise* scheme (with groupsizes $U = 2$ and $U = 4$) and the standard SC-MMSE FDE for scenario S1 and S2, respectively. As can be seen, similar performances are obtained by both turbo receivers for both subgroups when all users are spatially well separated (scenario S1). On the contrary, when users are spatially, closely, located and experience LOS propagation, as in scenario S2, the *groupwise* receiver clearly outperforms the standard receiver and achieves 1 dB and 6 dB gains at BER=10^{-2} for the groupsizes $U = 2$ and $U = 4$, respectively.

Fig. 9 illustrates the BER comparison for the *groupwise* receiver with MSE and correlation-based group selection for scenario S3. Similar to Fig. 8, we observe a performance gain of the *groupwise* receiver with increasing groupsize. Interestingly, we also observe that all three grouping schemes perform similar at the first iteration, whereas the simple static correlation-based grouping scheme (algorithm 3) yields a significant gain over the static MSE-based scheme (algorithm 2) at the last turbo iteration. This indicates that group selection based on the MSE criterion at the first iteration may not be optimal for the overall iterative process. The results in Fig. 9 also show that the simple correlation-based grouping (algorithm 3) achieves similar performance than the dynamic MSE-based scheme (algorithm 1) at a reduced complexity.

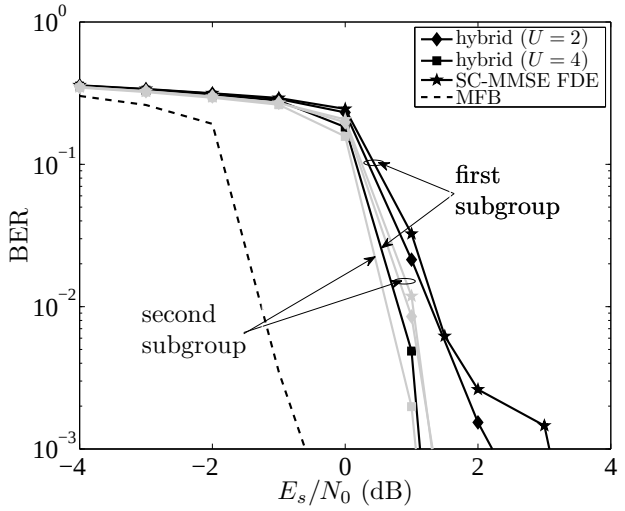

(a)

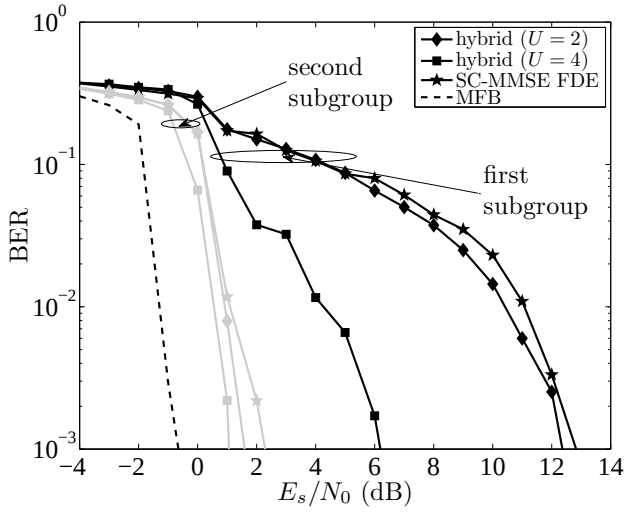

(b)

Fig. 8. Average BER performance for the two subgroups (black: first subgroup (user 1 to 4)), gray: second subgroup (user 5 to 8)) of the hybrid scheme and the standard SC-MMSE FDE for an $N = M = 8$ multiuser system for (a) scenario S1 and (b) scenario S2.

VII. Conclusion

A novel turbo equalization scheme based on a group separation strategy has been proposed in this paper as a framework for multiple access single carrier block transmission. The novel turbo equalizer offers a great design flexibility in terms of complexity and robustness against spatial channel correlation. The correlation chart analysis and BER performance evaluation have confirmed that the novel frequency domain *groupwise* turbo scheme achieves for a moderately chosen group size a considerable performance gain compared to the standard SC-MMSE FDE in channels with high spatial correlation among the users' signals. We have also developed three new GS algorithms based on MSE and channel correlation criteria for group selection. By a realistic channel sounding data based performance evaluation it has been demonstrated that the simple static correlation-based GS algorithm achieves similar performance than the dynamic MSE-based method at a significantly reduced complexity.

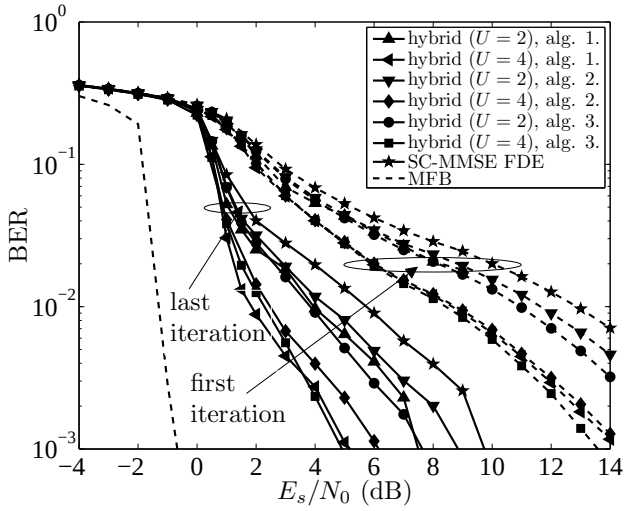

Fig. 9. Average BER performance of the hybrid scheme and the standard SC-MMSE FDE for scenario S3.

VIII. Acknowledgment

The authors would like to thank the reviewers for their comments which helped to improve the paper.

Appendix A
Lagrangian for Groupwise MSE Criterion

The optimization problem in (19) is obviously convex. Thus, it has a unique solution given in terms of the Karush-Kuhn-Tucker (KKT) conditions applied to the Lagrangian function

$$\mathcal{L}(\hat{\mathbf{\Gamma}}_g, \boldsymbol{\lambda}) = Q^{-1}\text{Trace}\,\big(\hat{\mathbf{\Gamma}}_g^H \mathbf{\Sigma}_0 \hat{\mathbf{\Gamma}}_g\big) + \boldsymbol{\lambda}^T\big(Q^{-1}\text{diag}(\hat{\mathbf{\Gamma}}_g^H \mathbf{\Upsilon}_g) - \mathbf{1}_U\big), \quad (36)$$

where $\boldsymbol{\lambda} = [\lambda_1, ..., \lambda_U]^T$ is a vector containing the Lagrangian multipliers. Let $\hat{\boldsymbol{\gamma}}_{g,u}$ be the u column of $\hat{\mathbf{\Gamma}}_g$. The optimization of (36) is equivalent to the optimization of the individual component-cost functions, indexed by u, separately. Therefore, Eqn. (36) also be written as

$$\mathcal{L}(\hat{\mathbf{\Gamma}}_g, \boldsymbol{\lambda}) = \sum_{u=1}^{U} \Big(Q^{-1} \hat{\boldsymbol{\gamma}}_{g,u}^H \mathbf{\Sigma}_0 \hat{\boldsymbol{\gamma}}_{g,u} + \lambda_u \big(Q^{-1} \hat{\boldsymbol{\gamma}}_{g,u}^H \mathbf{\Upsilon}_g \mathbf{e}_u - 1 \big) \Big). \quad (37)$$

The KKT conditions to (37) are given by

$$Q^{-1}\mathbf{\Sigma}_0 \hat{\boldsymbol{\gamma}}_{g,u} + Q^{-1}\lambda_u \mathbf{\Upsilon}_g \mathbf{e}_u = \mathbf{0}, \forall u, \quad (38)$$

$$Q^{-1}\mathbf{e}_u^T \mathbf{\Upsilon}_g^H \hat{\boldsymbol{\gamma}}_{g,u} - 1 = 0, \forall u. \quad (39)$$

After some straightforward manipulations of (38) and (39), the optimal frequency domain filter for the uth component is obtained as

$$\hat{\boldsymbol{\gamma}}_{g,u} = Q\big(\mathbf{e}_u^T \mathbf{\Upsilon}_g^H \mathbf{\Sigma}_0^{-1} \mathbf{\Upsilon}_g \mathbf{e}_u\big)^{-1} \mathbf{\Sigma}_0^{-1} \mathbf{\Upsilon}_g \mathbf{e}_u. \quad (40)$$

Finally, applying the matrix-inversion lemma to (40) and rewriting the result in matrix-notation yields the expression in (20).

APPENDIX B
GROUPWISE FILTER COEFFICIENTS FOR SINR CRITERION

In this subsection, we derive the optimal filter weights solving the SINR criterion (29). The SINR for the gth subgroup can be expressed as

$$\begin{aligned}\text{SINR}_g &\equiv \frac{\mathbb{E}\big[\,\|\mathbf{M}_g\mathbf{c}_g(k)\|^2\,\big]}{\mathbb{E}\big[\,\|\mathbf{z}_g(k)-\mathbf{M}_g\mathbf{c}_g(k)\|^2\,\big]}\\ &= \frac{\text{Trace}\left(\mathbf{M}_g\mathbf{M}_g^H\right)}{\text{Trace}\left(\begin{array}{c}\left(\mathbf{W}_g^H\overline{\mathbf{H}}_g-\mathbf{M}_g\right)\boldsymbol{\Lambda}_g^{(1)}\left(\mathbf{W}_g^H\overline{\mathbf{H}}_g-\mathbf{M}_g\right)^H\\ +\mathbf{W}_g^H\,\overline{\overline{\mathbf{H}}}_g\boldsymbol{\Lambda}_g^{(2)}\overline{\overline{\mathbf{H}}}_g^H\mathbf{W}_g+\mathbf{W}_g^H\mathbf{W}_g\end{array}\right)}\\ &= \frac{\text{Trace}\left(\left(\mathbf{U}_g\otimes\mathbf{I}_U\right)\left(\mathbf{U}_g\otimes\mathbf{I}_U\right)^H\right)}{\text{Trace}\left(\boldsymbol{\Gamma}_g^H\boldsymbol{\Sigma}\boldsymbol{\Gamma}_g-\mathbf{M}_g\boldsymbol{\Lambda}_g^{(1)}\mathbf{M}_g^H\right)}\\ &= \frac{\text{Trace}\left(\hat{\boldsymbol{\Gamma}}_g^H\boldsymbol{\Upsilon}_g\boldsymbol{\Upsilon}_g^H\hat{\boldsymbol{\Gamma}}_g\right)}{\text{Trace}\left(\hat{\boldsymbol{\Gamma}}_g^H\left(Q\boldsymbol{\Sigma}-\boldsymbol{\Upsilon}_g\hat{\boldsymbol{\Lambda}}_g\boldsymbol{\Upsilon}_g^H\right)\hat{\boldsymbol{\Gamma}}_g\right)}. \end{aligned} \tag{41}$$

Based on (41), the problem of maximizing the SINR for each subgroup can be written as

$$\breve{\boldsymbol{\Gamma}}_g = \arg\max_{\{\hat{\boldsymbol{\Gamma}}_g\in\mathbb{C}^{U\times MQ}\}}\frac{\text{Trace}\left(\hat{\boldsymbol{\Gamma}}_g^H\mathbf{Z}_{g,1}\hat{\boldsymbol{\Gamma}}_g\right)}{\text{Trace}\left(\hat{\boldsymbol{\Gamma}}_g^H\mathbf{Z}_{g,2}\hat{\boldsymbol{\Gamma}}_g\right)}, \tag{42}$$

where $\mathbf{Z}_{g,1}\equiv\boldsymbol{\Upsilon}_g\boldsymbol{\Upsilon}_g^H\in\mathbb{C}^{QM\times QM}$ and $\mathbf{Z}_{g,2}\equiv Q\boldsymbol{\Sigma}-\boldsymbol{\Upsilon}_g\hat{\boldsymbol{\Lambda}}_g\boldsymbol{\Upsilon}_g^H\in\mathbb{C}^{QM\times QM}$ are Hermitian and Hermitian positive definite, respectively. Therefore, Eqn. (42) can be expressed as a generalized eigenvalue problem, where the matrices $\mathbf{Z}_{g,1}$ and $\mathbf{Z}_{g,2}$ can be jointly diagonalized as [35]

$$\mathbf{X}_g^H\mathbf{Z}_{g,1}\mathbf{X}_g=\mathbf{Q}_g \tag{43}$$

$$\mathbf{X}_g^H\mathbf{Z}_{g,2}\mathbf{X}_g=Q^2\mathbf{I}_U. \tag{44}$$

Here, $\mathbf{Q}_g=\text{diag}\{t_{g,1},t_{g,2},...,t_{g,U},0,...0\}$ is an $QM\times QM$ diagonal matrix, containing the generalized nonnegative eigenvalues $t_{g,1}\geq t_{g,2}\geq...\geq t_{g,U}$ listed in decreasing order, and $\mathbf{X}_g$ is the matrix of the corresponding generalized eigenvectors. Then, the optimal filter corresponds to the first U columns of $\mathbf{X}_g$. Similar to [22], the solution to (42) can be found by applying the Cholesky factorization to $\mathbf{Z}_{g,2}$, $\mathbf{Z}_{g,2}=\mathbf{C}_g^H\mathbf{C}_g$, and solving the standard eigenvalue problem

$$Q^2\mathbf{C}_g^{-H}\mathbf{Z}_{g,1}\mathbf{C}_g^{-1}=\mathbf{E}_g\mathbf{Q}_g\mathbf{E}_g^H, \tag{45}$$

where $\mathbf{E}_g\in\mathcal{C}^{QM\times QM}$ is unitary. The optimal filter maximizing the above ratio is then given by

$$\breve{\boldsymbol{\Gamma}}_g=Q\mathbf{C}_g^{-1}\mathbf{T}_g, \tag{46}$$

where $\mathbf{T}_g\in\mathbb{C}^{QM\times U}$ consists of the first U eigenvectors of $\mathbf{E}_g$ corresponding to the U nonzero eigenvalues of $\mathbf{Q}_g$. Moreover, the SINR related to the gth subgroup is found to

$$\text{SINR}_g=\frac{1}{UQ^2}\sum_{u=1}^{U}t_{g,u}. \tag{47}$$

Also, the equivalent channel and covariance matrices of the filter output signal $\mathbf{z}_{g,q}(k)$ in (24), respectively, are obtained as

$$\breve{\mathbf{U}}_g=Q^{-1}\mathbf{T}_g^H\mathbf{C}_g^{-H}\boldsymbol{\Upsilon}_g \text{ and } \breve{\mathbf{R}}_g=\mathbf{I}_U. \tag{48}$$

From (48), we observe that the *groupwise* frequency domain SINR filter (46) is a noise-whitening filter that whitens the residual interference plus noise term.

APPENDIX C
PROOF OF THEOREM 3.4

To prove that the MSE and SINR criteria (17) and (29) lead to the same MAP decision metric $\rho_{g,q}(k)$, we first explicitly express $\rho_{g,q}(k)$ as a function of the filter $\hat{\boldsymbol{\Gamma}}_g$ and covariance matrix $\mathbf{R}_g$. By noting that $\mathbf{z}_{g,q}(k)$ in (24) is given by $\mathbf{z}_{g,q}(k)=\mathbf{S}_q\mathbf{F}_U^H\boldsymbol{\Gamma}_g^H\underline{\breve{\mathbf{r}}}(k)+\mathbf{U}_g\bar{\mathbf{c}}_{g,q}(k)$, the MAP decision metric (27) can be written as

$$\begin{aligned}\rho_{g,q}(k) &= -\left(\mathbf{z}_{g,q}(k)-\mathbf{U}_g\mathbf{x}\right)^H\mathbf{R}_g^{-1}\left(\mathbf{z}_{g,q}(k)-\mathbf{U}_g\mathbf{x}\right)\\ &= \left(\mathbf{S}_q\mathbf{F}_U^H\boldsymbol{\Gamma}_g^H\underline{\breve{\mathbf{r}}}(k)-\mathbf{U}_g(\mathbf{x}-\bar{\mathbf{c}}_{g,q}(k))\right)^H\mathbf{R}_g^{-1}\\ &\quad\times\left(\mathbf{S}_q\mathbf{F}_U^H\boldsymbol{\Gamma}_g^H\underline{\breve{\mathbf{r}}}(k)-\mathbf{U}_g(\mathbf{x}-\bar{\mathbf{c}}_{g,q}(k))\right).\end{aligned} \tag{49}$$

The matrix product $\mathbf{S}_q\mathbf{F}_U^H\boldsymbol{\Gamma}_g^H$ is obviously equivalent to the product $\hat{\boldsymbol{\Gamma}}_g^H\mathbf{D}_q^H$, where $\mathbf{D}_q\equiv\left(\mathbf{I}_M\otimes\text{diag}\{\mathbf{e}_q^T\mathbf{F}\}\right)$. Moreover, since $\mathbf{U}_g=Q^{-1}\hat{\boldsymbol{\Gamma}}_g^H\boldsymbol{\Upsilon}_g$, we can further write (49) as

$$\begin{aligned}\rho_{g,q}(k) &= \left(\mathbf{D}_q^H\underline{\breve{\mathbf{r}}}(k)-Q^{-1}\boldsymbol{\Upsilon}_g\left(\mathbf{x}-\bar{\mathbf{c}}_{g,q}(k)\right)\right)^H\hat{\boldsymbol{\Gamma}}_g\mathbf{R}_g^{-1}\\ &\quad\times\hat{\boldsymbol{\Gamma}}_g^H\left(\mathbf{D}_q^H\underline{\breve{\mathbf{r}}}(k)-Q^{-1}\boldsymbol{\Upsilon}_g\left(\mathbf{x}-\bar{\mathbf{c}}_{g,q}(k)\right)\right).\end{aligned} \tag{50}$$

Consequently from (50), we see that it remains to show that the matrix product

$$\mathbf{Y}_g\equiv\hat{\boldsymbol{\Gamma}}_g\mathbf{R}_g^{-1}\hat{\boldsymbol{\Gamma}}_g^H \tag{51}$$

is identical for the MSE and SINR criteria. For the MSE criterion (17), $\mathbf{Y}_g$ in (51) can be expressed with (20) and (25) as

$$\begin{aligned}\mathbf{Y}_g &= \breve{\boldsymbol{\Gamma}}_g\mathbf{R}_g^{-1}\breve{\boldsymbol{\Gamma}}_g^H\\ &= \left(\boldsymbol{\Sigma}^{-1}\boldsymbol{\Upsilon}_g\boldsymbol{\Theta}_g^{-1}\boldsymbol{\Omega}_g^{-1}\right)\left(Q^{-1}\boldsymbol{\Omega}_g^{-1}\boldsymbol{\Theta}_g^{-1}\boldsymbol{\Upsilon}_g^H\boldsymbol{\Sigma}^{-1}\boldsymbol{\Upsilon}_g\boldsymbol{\Omega}_g^{-1}\right)^{-1}\\ &\quad\times\left(\boldsymbol{\Sigma}^{-1}\boldsymbol{\Upsilon}_g\boldsymbol{\Theta}_g^{-1}\boldsymbol{\Omega}_g^{-1}\right)^H\\ &= Q\boldsymbol{\Sigma}^{-1}\boldsymbol{\Upsilon}_g\boldsymbol{\Theta}_g^{-1}\left(\boldsymbol{\Upsilon}_g^H\boldsymbol{\Sigma}^{-1}\boldsymbol{\Upsilon}_g\right)^{-1}\boldsymbol{\Upsilon}_g^H\boldsymbol{\Sigma}^{-1}.\end{aligned} \tag{52}$$

Let us now compute $\hat{\boldsymbol{\Gamma}}_g\mathbf{R}_g^{-1}\hat{\boldsymbol{\Gamma}}_g^H$ for the SINR formulation (17). Using the filter in (46) and the covariance matrix in (48), we get

$$\breve{\boldsymbol{\Gamma}}_g\breve{\mathbf{R}}_g^{-1}\breve{\boldsymbol{\Gamma}}_g^H=Q^2\mathbf{C}_g^{-1}\mathbf{T}_g\mathbf{T}_g^H\mathbf{C}_g^{-H}. \tag{53}$$

From (45), we have

$$\mathbf{T}_g\mathbf{T}_g^H=Q^4\mathbf{C}_g^{-H}\mathbf{Z}_{g,1}\mathbf{C}_g^{-1}\mathbf{T}_g\hat{\mathbf{Q}}_g^{-2}\mathbf{T}_g^H\mathbf{C}_g^{-H}\mathbf{Z}_{g,1}^H\mathbf{C}_g^{-1} \tag{54}$$

and

$$\hat{\mathbf{Q}}_g^{-1}=Q^{-2}\left(\boldsymbol{\Upsilon}_g^H\mathbf{C}_g^{-1}\mathbf{T}_g\right)^{-1}\left(\mathbf{T}_g^H\mathbf{C}_g^{-H}\boldsymbol{\Upsilon}_g\right)^{-1}, \tag{55}$$

where $\hat{\mathbf{Q}}_g=\text{diag}\{t_{g,1},t_{g,2},...,t_{g,U}\}$ is the $U\times U$ diagonal matrix containing the U nonzero diagonal elements of $\mathbf{Q}_g$.

Substituting (54) and (55) into (53) and using simple algebra, we have

$$\begin{aligned}&\check{\mathbf{\Gamma}}_g\mathbf{R}_g^{-1}\check{\mathbf{\Gamma}}_g^H\\&= Q^2\mathbf{Z}_{g,2}^{-1}\mathbf{\Upsilon}_g\big(\mathbf{\Upsilon}_g^H\mathbf{Z}_{g,2}^{-1}\mathbf{\Upsilon}_g\big)^{-1}\mathbf{\Upsilon}_g^H\mathbf{Z}_{g,2}^{-1}.\end{aligned}$$

Now, applying the matrix inversion lemma to $\mathbf{Z}_{g,2}^{-1}\mathbf{\Upsilon}_g$, we obtain

$$\begin{aligned}&\check{\mathbf{\Gamma}}_g\mathbf{R}_g^{-1}\check{\mathbf{\Gamma}}_g^H\\&= Q\mathbf{\Sigma}^{-1}\mathbf{\Upsilon}_g\mathbf{\Theta}_g^{-1}\big(\mathbf{\Upsilon}_g^H\mathbf{\Sigma}^{-1}\mathbf{\Upsilon}_g\big)^{-1}\mathbf{\Upsilon}_g^H\mathbf{\Sigma}^{-1}\\&= \mathbf{Y}_g,\end{aligned}$$

which is identical to (52).

REFERENCES

[1] S. Verdu, "Multiuser Detection," *Cambridge University Press*, 1998.

[2] C. Douillard, et al., "Iterative correction of intersymbol interference: Turbo equalization," *European Trans. Telecomm.*, vol. 6, pp. 507-511, Sept. 1995.

[3] X. Wang, and H. V. Poor, "Iterative (turbo) soft interference cancellation and decoding for coded CDMA," *IEEE Trans. Commun.*, vol. 47, pp. 1046-1061, July 1999.

[4] M. Tüchler, R. Koetter, and A. C. Singer, "Turbo equalization: principles and new results," *IEEE Trans. Commun.*, vol. 50, pp. 754-767, May 2002

[5] M. Tüchler, R. Koetter, and A. C. Singer, "Minimum mean squared error equalization using a priori information," *IEEE Trans. Signal Processing*, vol. 50, no. 3, pp. 673-683, March 2002

[6] T. Abe, and T. Matsumoto, "Space-time turbo equalization in frequency-selective MIMO channels," *IEEE Trans. Veh. Techn.*, vol. 52, no. 3, pp. 469-475, May 2003.

[7] M. Tüchler, and J. Hagenauer, "Turbo equalization using frequency domain equalizers," *in Proc. of Allerton Conference*, Monticello, IL, USA, Oct. 2000.

[8] P. Schniter, and H. Liu, "Iterative frequency-domain equalization for single-carrier systems in doubly-dispersive channels," *in Proc. Asimolar Conf. Signals, Syst., Comp.*, vol 1, pp. 667-671, Nov. 2004.

[9] Y. Wu, X. Zhu, and A. K. Nandi, "Low complexity Turbo space frequency equalization for single-carrier MIMO wireless communications," *in Proc. EUSIPCO '06*, Florence, Italy, Sept. 2006.

[10] K. Kansanen, and T. Matsumoto, "An analytical method for MMSE MIMO turbo equalizer EXIT chart computation," *IEEE Trans. Wireless Commun.*, vol. 6, no. 1, pp. 59-63, Jan. 2007.

[11] K. Amis, L. Josse, and C. Laot, "Efficient frequency-domain MMSE turbo equalization derivation and performance comparison with the time-domain counterpart," *in Proc. ICWMC '07*, Guadeloupe, France, pp. 65-69, Mar. 2007.

[12] X. Yuan, Q. Guo, X. Wang, and L. Ping, "Evolution Analysis of Low-Cost Iterative Equalization in Coded Linear Systems with Cyclic Prefixes," *IEEE J. Sel. Areas Commun.*, vol. 26, pp. 301-310, Feb. 2008.

[13] J. Choi, "A Correlation Based Analysis for Approximate MAP Detectors and Iterative Receivers," *IEEE Trans. Wireless Commun.*, vol. 6, no. 5, pp. 1764-1773, May 2007.

[14] A. Elkhazin, K. N. Plataniotis, and S. Pasupathy, "Reduced-dimension MAP turbo-BLAST detection," *IEEE Trans. Commun.*, vol. 54, pp. 108-118, Jan. 2006.

[15] N. Veselinovic, T. Matsumoto, and M. Juntti, "Iterative MIMO Turbo Multiuser Detection and Equalization for STTrC-Coded Systems with Unknown Interference," *EURASIP J. Wireless Commun. and Networking*, vol. 2, pp. 309-321, Dec. 2004.

[16] M. Grossmann, and T. Matsumoto, "Hybrid Turbo Multiuser Detection for OFDM Transmission with Spatially-Correlated Channels," *IEEE Commun. Letters*, vol. 11, pp. 420-422, May 2007.

[17] R. Visoz, A. O. Berthet, and S. Chtourou, "Frequency-Domain Block Turbo-Equalization for Single-Carrier Transmission Over MIMO Broadband Wireless Channel," *IEEE Trans. Wireless Commun.*, vol. 54, no. 12, pp. 2144-2149 , Dec. 2006.

[18] M. Grossmann, and T. Matsumoto, "Nonlinear Frequency Domain MMSE Turbo Equalization using Probabilistic Data Association," *IEEE Commun. Letters*, vol. 12, pp. 295-297, April 2008.

[19] M. Grossmann, "Outage Performance Analysis and Code Design for Three-Stage MMSE Turbo Equalization in Frequency-Selective Rayleigh Fading Channels," *IEEE Trans. Veh. Technology* , vol. 60, no. 2, pp. 473-484, Feb. 2011.

[20] M. K. Varanasi, "Group detection for synchronous Gaussian code-division multiple-access channels," *IEEE Trans. Inform. Theory*, vol. 41, pp. 1083-1096, July 1995.

[21] X. Li, H. C. Huang, A. Lozano, and G. J. Foschini, "Reduced-complexity detection algorithms for systems using multi-element arrays," *in Proc. IEEE GLOBECOM '00*, vol. 2, pp. 1072-1076, Nov. 2000.

[22] S.H. Moon, J. Jeong, H. Lee, and I. Lee, "Enhanced Groupwise Detection with a New Receive Combiner for Spatial Multiplexing MIMO Systems," *IEEE Trans. Commun.*, vol. 58, pp. 2511-2515, Sept. 2010.

[23] J. P. Kermoal, L. Schumacher, K. I. Pedersen, P. E. Mogensen, and F. Frederiksen, "A stochastic MIMO radio channel model with experimental validation," *IEEE J. Sel. Areas Commun.*, vol. 20, pp. 1211-1226, Aug. 2002.

[24] C. Laot, R. Le Bidan, and D. Leroux, "Low-complexity MMSE turbo equalization: A possible solution for EDGE," *IEEE Trans. Wireless Commun.*, vol. 4, pp. 965-974, May 2005.

[25] G. Caire, R. R. Mueller, and T. Tanaka, "Iterative multiuser joint decoding: optimal power allocation and low-complexity implementation," *IEEE Trans. Inform. Theory*, vol. 50, no. 9, pp. 1950-1973 , Sept. 2004.

[26] S. ten Brink, "Convergence behavior of iteratively decoded parallel concatenated codes," *IEEE Trans. Commun.*, vol. 49, pp. 1727-1737, Oct. 2001.

[27] J. Boutros, N. Gresset, L. Brunel, and M. Fossorier, "Soft-input soft-output lattice sphere decoder for linear channels," *in Proc. IEEE GLOBECOM '03*, vol. 3, pp. 1583-1587, Dec. 2003.

[28] A. Kammoun, M. Kharouf, W. Hachem, and J. Najim, "BER and Outage Probability Approximations for LMMSE Detectors on Correlated MIMO Channels," *IEEE Trans. Inform. Theory*, vol. 55, pp. 4386-4397 , Oct. 2009.

[29] F. Brännström, L.K. Rasmussen, and A.J. Grant, "Convergence analysis and optimal scheduling for multiple concatenated codes," *IEEE Trans. Inform. Theory*, vol. 51, pp. 3354-3364, Sept. 2005.

[30] E. Kreyszig, "Advanced Engineering Mathematics," *9th ed. John Wiley & Sons*, New York, 2005.

[31] J. Jeong, H. Lee, S.H. Moon, and I. Lee, "Enhanced Group Detection with a New Receiver Combiner for Spatial Multiplexing MIMO systems," *in Proc. IEEE Veh. Technol. Conf. Fall 2008*, Calgary, CANADA, Sept. 2008, pp. 1-5.

[32] M. Tuechler, "Design of serially concatenated systems depending on the block length," *IEEE Trans. Comm.*, vol. 52, pp. 209-218, Feb. 2004.

[33] U. Trautwein, C. Schneider, and R. Thomae, "Measurement Based Performance Evaluation of Advanced MIMO Transceiver Designs," *EURASIP Journal on Applied Signal Processing*, pp. 1712-1724, Jan. 2005.

[34] "WINNER II channel models," *Tech. Rep. IST-4-027756 WINNER II D1.1.2 V1.2*, Feb. 2008.

[35] M. Sadek, A. Tarighat, and A. H. Sayed, "A leakage-based precoding scheme for downlink multi-user MIMO channels," *IEEE Trans. Wireless Commun.*, vol. 6, no. 5, pp. 1711-1721, May 2007.

Marcus Grossmann received the Diplom-Ingenieur (M.S.) degree in electrical engineering and computer science in 2004 from Ilmenau University of Technology, Ilmenau, Germany. From 2005 to 2010, he was with the Institute for Information Technology at Ilmenau University of Technology. In 2011, he joined the Fraunhofer Institute for Integrated Circuits, Ilmenau, Germany.

His research interests are communication systems and signal processing for wireless communications.

Christian Schneider received the Diplom-Ingenieur (M.S.) degree in electrical engineering from the Ilmenau University of Technology, Ilmenau, Germany in 2001. He is currently pursuing the Dr.-Ing. degree with the Institute for Information Technology at the Ilmenau University of Technology.

His research interests are space-time signal processing, turbo techniques, adaptive techniques, multi dimensional channel sounding, channel characterization and analysis as well as channel modelling.